INVESTIGATION OF THE STRUCTURAL BEHAVIOUR OF MEGALITHIC MNAJDRA MONUMENT

by

Siphesihle Mpho Motsa

Submitted in fulfilment of the requirements for the degree of
Master of Science in Engineering

School of Civil Engineering, Surveying and Construction
University of KwaZulu-Natal
Durban
November 2018

Examiner's copy

ABSTRACT

The Maltese megalithic temples are regarded as one of the oldest structures from early civilization dating back to about the 4th millennium. These megalithic structures provide valuable information due to their complexity of geometry and the way they were constructed, and they also serve as one of the main tourist attraction areas in the Maltese islands. The areas in which these megalithic structures are found have been listed as UNESCO World Heritage Sites.

In this study, the structural behaviour of the middle temple of the Mnajdra megalithic temple is investigated. First, the geometry of the temple was obtained from a cloud of points using radar-laser scanning. The mechanical material properties of the megaliths and soil were obtained from published experimental research on similar monuments. A finite element model was created whereby nonlinear contact mechanics was applied since unilateral contact between parts is the major stress-transfer mechanism. Simulations from eigenmode analysis show various natural frequencies and shape modes of the monument which can be validated from experimental data obtained from an ambient vibration monitor. Results obtained from structural analysis show the major stress transfer points between the megaliths, the response of the structure under selected loading scenarios as well as potential collapse mechanisms.

DECLARATION- PLAGIARISM

Supervisor:

As the candidate's supervisor, I agree to the submission of this dissertation.

Signed: ……..…... **Dr. Georgios A. Drosopoulos** Date: ……

Candidate:

I,. **Siphesihle Mpho Motsa ,** declare that

1. The research reported in this dissertation, except where otherwise indicated, is my original research.

2. This dissertation has not been submitted for any degree or examination at any other university.

3. This dissertation does not contain other persons' data, pictures, graphs or other information, unless specifically acknowledged as being sourced from other persons.

4. This dissertation does not contain other persons' writing, unless specifically acknowledged as being sourced from other researchers. Where other written sources have been quoted, then:

a. Their words have been re-written, but the general information attributed to them has been referenced

b. Where their exact words have been used, then their writing has been placed in italics and inside quotation marks and referenced

5. This dissertation does not contain text, graphics or tables copied and pasted from the Internet, unless specifically acknowledged, and the source being detailed in the thesis and in the References sections.

Signed:

…… ……..……

Siphesihle Mpho Motsa Date

Page intentionally left blank

ACKNOWLEDGEMENTS

Firstly, all praise and thanks to the **Almighty** for providing me with the capacity and resources to conduct this research.

Secondly, I would like to express my sincerest grateful to my parents who have sacrificed so much to enable me to attend university and follow my dreams. Their continued support throughout my studying career has been inspiring.

Thirdly, **Dr Georgios A. Drosopoulos** deserve a special vote of thanks for his supervision, guidance, discussions and great insight in the field of structural Engineering & computational mechanics. He has provided assistant to me in more ways than he should and has gone beyond the role of a supervisor; for this, I am extremely grateful.

Lastly, special acknowledgements to **Dr. Ruben Paul Borg**, University of Malta, and his team for providing experimental data for the geometry and vibration behaviour of the monument which is investigated in this thesis.

"Luck is the dividend of sweat. The more you sweat, the luckier you get"

Raymond Albert Kroc

Contents

List of Figures

List of Tables

This dissertation is prepared in the form of an article which is about to be submitted for publication in an international journal.

This article has been created with the contribution of the following co-authors, which are about to participate in the publication: Siphesihle Mpho Motsa, Georgios A. Drosopoulos, Maria Stavroulaki, Manolis Maravelakis, Ruben Paul Borg, Pauline Galea, Sebastiano d'Amico and Georgios Stavroulakis.

Georgios A. Drosopoulos is the supervisor of this master. Maria Stavroulaki and Georgios Stavroulakis have contributed to the research by several discussions and advices on the topic. Manolis Maravelakis has advised on the experimental data obtained from University of Malta for the geometry of the monument. Ruben Paul Borg, Pauline Galea, and Sebastiano d'Amico have provided the experimental data which are compared with the numerical models developed in this work.

Investigation of the structural behaviour of megalithic Mnajdra monument

Abstract

The Maltese megalithic temples are regarded as one of the oldest structures from early civilization dating back to about the 4th millennium. These megalithic structures provide valuable information due to their complexity of geometry and the way they were constructed, and they also serve as one of the main tourist attraction areas in the Maltese islands. The areas in which these megalithic structures are found have been listed as UNESCO World Heritage Sites. In this study, the structural behaviour of the middle temple of the Mnajdra Megalithic temple is investigated. First, the geometry of the temple was obtained from a cloud of points using radar-laser scanning. The mechanical material properties of the megaliths and soil were obtained from published experimental research on similar monuments. A finite element model was created whereby nonlinear contact mechanics was applied since unilateral contact between parts is the major stress-transfer mechanism. Simulations from eigenmode analysis show various natural frequencies and shape modes of the monument which can be validated from experimental data obtained from an ambient vibration monitor. Results obtained from structural analysis show the major stress transfer points between the megaliths, the response of the structure under selected loading scenarios as well as potential collapse mechanisms.

Keywords: megalithic monuments; unilateral contact-friction; dynamic analysis; damage; Mnajdra

1. Introduction

The Mnajdra stone temple is one of the megalithic temples located in the islands of Malta and Gozo (Galdies, 2011, Cassar, 2002). Megalithic is a term used to describe these Neolithic structures which are made of large Globigerina (*Franka)* and Lower Coralline (*Zonqor*) limestones (Torpiano, 2011). The Globigerina limestone which is locally known as *Franka* makes up the internal spaces and walls of the temple and the Lower Coralline limestone which is locally known as *Zonqor* makes up the external walls of the temple (Cassar, 2010, Bianco, 1999). Megalithic temples are believed to be among the oldest archaeological stone monuments in the world dating back to the 4th millennium BC (Sammut, 2016). Thus, they are older than the famous Stonehenge monument located in England and the Great Pyramid of Giza, Egypt (Bianco, 2017).

The Mnajdra temple is one of the best preserved out of five temples (namely, Ta'Hagrat, Skorba, Ħaġar Qim,Tarxien and Mnajdra) in the island of Malta (White, 2018, Ridley, 1971). These megalithic temples have been listed under the UNESCO's World Heritage List of six prehistoric monumental complexes, including the Ġgantija temple in Gozo Island (Cassar et al., 2018).

Research by Torpiano (1995) has shown that rainfall is one of the reasons which causes structural failure of the monument. In 1995, parts of the Mnajdra temple collapsed due to heavy rainfall, which caused an increase in the backfill pressure exerted on the megalithic wall (Torpiano, 1995).Weather and climate conditions also affect the structural integrity of the monuments, mainly by chemical degradation of the limestones (Cassar et al., 2018). During the centuries, high temperatures (up to 40°C) (Galdies, 2011, Ramírez-Cisneros et al., 2012), excessive winds and sunlight exposure have also contributed to this deterioration of the structural integrity of the megaliths and surrounding structures: powdering, flaking, honeycombing and scaling of the stone surface have been observed (Cassar, 2002, Vannucci et al., 1994, Cassar et al., 2018).

A number of the megaliths have been infested with cracks and breaks due to rotation and collapse of other megaliths. This results in a gradually increased pressure applied on dependent stones, which eventually creates damage to them (Cassar, 2002). Deterioration phenomena become more severe by the accumulation of soil in the backfill, growth of vegetation in the megaliths which results in cracks and/or widening of existing cracks, and salt crystallisation which is accelerated by windy weather conditions (Fitzner et al., 1997, Cassar et al., 2011, Cassar et al., 2018). In 2011 and 2009, some of the panels of the protection shelter covering the Ħaġar Qim and Mnajdra temples respectively, were ripped apart due to excessive winds, however, both temples were reported to be undamaged following these incidents (Malta, 2011, News, 2009). Other factors which contribute to the structural failure of the monument include vandalism and blasting from near-by quarries (Türer et al., 2012, Zanelli, 2015).

Due to the increased frequency of damage phenomena over the years, different techniques have been adopted to address these events. In 1910, the insertion of metal (iron) was used to hold together broken megaliths in the Ħaġar Qim temple (Cassar, 1988). In 1949, cement mixed with Globigerina Limestone chippings were used to restore the stones which were close to collapse (Evans, 1971). In the mid-1970s, linseed oil was applied every summer to the megaliths to minimize the influence of the weather conditions (Cassar, 1988). In 1994, following the collapse of parts of the Mnajdra temple, a new wall with concrete bricks was constructed behind the original megalithic wall to retain the soil backfill and to prevent excessive pressure on the megaliths. In addition, a rainwater drainage system was installed in the central temple of Mnajdra (Cassar, 1988). In 2008 temporal protective shelters were constructed over Hager Qim and Mnajdra temples as a short-time solution to delay the rate of deterioration

To evaluate the structural response of historical masonry monuments, both numerical and experimental research have been conducted. Finite element analysis is widely recognized as an effective method for the structural assessment or restoration of old structures (Aguilar et al., 2017, Aktaş and Turer, 2015, Terzi and Ignatakis, 2018, Sánchez-Aparicio et al., 2014, Betti and Vignoli, 2008, Taliercio and Binda, 2007, Vercher et al., 2015). In particular, static and dynamic numerical finite element analysis is commonly used to assess the structural response of masonry structures. In this framework, several challenges are faced, depending on a number of parameters: (i) the structural complexity and geometry of the structure (Betti and Vignoli, 2011, Lourenço, 2002, Augusti et al., 2001, Mele et al., 2003); (ii) the material properties of the different elements that make up the structure (Mele et al., 2003); (iii) the nonlinear behaviour of the materials of masonry (Betti and Vignoli, 2011, Lourenço, 2002, Augusti et al., 2001, Ramírez-Cisneros et al., 2012); (iv) the existence of pathology, such as cracking following event of settlements and/or weathering deterioration (Sánchez-Aparicio et al., 2014, Reyes et al., 2008); (v) the uncertainty of material properties and geometry of structural elements (Betti and Galano, 2012, Casarin and Modena, 2006).

Due to these challenges, modelling or predicting the structural response of historical masonry structures can be more sophisticated than designing new structures (Del Piero, 1984, Carpinteri et al., 2005, Betti and Vignoli, 2008, Betti et al., 2016), due to uncertainties related to geometry and boundary conditions, material properties and load history of existing structures (Sánchez-Aparicio et al., 2014, Ramos et al., 2013). Finite element analysis has been been used to investigate the structural behaviour of a masonry castle (Frangokastello) in Greece, by considering the existing failure which consists of cracks and local failure of the masonry (Stavroulaki et al., 2018). A dynamic finite element analysis was conducted on the Nemrut monuments to investigate the effects of snow, wind, vandalism and blast (Türer et al., 2012). An inverse analysis procedure was proposed in Conde et al., 2016, to investigate pathological

problems on masonry arch bridges where nonlinear finite elements models were adopted based on the principles of non-smooth mechanics. More finite element models and their practical application can be found in (Cattari et al., 2014, Leftheris et al., 2006, Milani et al., 2013, Stavroulaki and Liarakos, 2012, Tiberti et al., 2016, Stavroulaki et al., 2016).

Experimental research can also substantially contribute to the evaluation of the structural response of existing masonry structures. Among several other techniques, an ambient vibration monitor can be used for collecting experiment data, usually for small structural movements which take place within a linear elasticity region (Pellegrini et al., 2018). This method has become one of the main experimental methods for assessing the dynamic response of full-scale structures since no excitation equipment is required (Sepe et al., 2008). The ambient vibration test has been used to determine the dynamic characteristics of reinforced concrete minarets in Firat University Engineering Campus Mosque (Bayraktar et al., 2010), assess structural conditions of the bell-tower of the Monza's Cathedral (Gentile and Saisi, 2007), assess the influence of the boundary conditions of a group of silos in the port of Antwerp (Dooms et al., 2006) as well as evaluate the structural integrity of bridges (Živanović et al., 2006, Bayraktar et al., 2007). Another technique which can be used to collect experimental data related to the dynamic response is the forced vibration test, where an excitation can be due to a vibrodyne and linear mass shaker (electrodynamic and servo hydraulic shakers) (Vestroni et al., 1996). This method was implemented on the structural assessment study of a two storey masonry house (Vestroni et al., 1996) and an old masonry house (Capecchi and Vestroni, 1991).

Ideally, experimental and numerical results can be combined in order to verify the structural performance of monuments. In particular, results obtained from eigenmode finite element analysis, such as natural frequencies and shape modes, can be compared to experimental research, in order to verify the validity of the material properties and other assumptions considered in the model (Aktaş and Turer, 2015, Vestroni et al., 1996).

In this study, an eigenmode analysis was initially conducted and a parametric assessment was carried out to assess the mechanical properties of the megaliths used in the model. To validate the model, the results obtained from the eigenmode simulations are compared to experiment results provided by ambient vibration monitors. The experimental data have been obtained from (Borg et al., 2018) are used, to create the geometry of the monument from a set of point clouds and to verify the developed numerical models. After the model was validated, a general nonlinear static structural analysis was conducted whereby settlement of supports is examined. Since some seismic activities have been recorded in the area surrounding the Malta region, (Spampinato et al., 2017), a dynamic analysis was finally conducted to investigate the effect of the earthquakes on the structure. Goal of the present work, is to provide an overall framework for the investigation

of the structural performance of ancient stone monuments, using experimental data, numerical analysis and past events depicting damage of the structure.

2. Description of monument

The megalithic Mnajdra temple is a complex which consists of three temples, among which the middle, is in the best-preserved state compared to the other temples (Figure 1). The Mnajdra temple is located about 500 metres from the Ħaġar Qim megalithic temple on the southern coast of the island of Malta and about 200 metres away from the coast making it more susceptible to weathering and chemical degradation. In Figure 2, positions for the rest of the megalithic structures of the islands of Gozo and Malta are shown. The middle temple is made up of four-apses which are shown in Figure 1 and has its pillar-stones decorated with marks drilled on the inner surface in horizontal rows (Figure 4).

The Globigerina limestone has been used for the internal walls of the Mnajdra temple since it is soft and can easily be carved. For these reasons it was regarded as the material of choice for buildings and decorations by the locals (Cassar, 2010). The Lower Coraline limestone makes up the external walls since it is harder, not easily eroded and presents greater durability (Cassar, 2010). The external and inner walls act as retaining walls for supporting the soil material and debris surrounding the walls (Figure 3). The limestones have no mortar in-between them, thus, friction is the major resisting mechanism.

Figure 1: Aerial view of the Mnajdra temple showing the three temples that make up the complex (NUNISMAG, 2018).

Figure 2: Map of Megalithic Temples of Malta (Theuma and Grima, 2006)

Figure 3: Picture showing the internal wall and part of the soil and debris retained by the middle temple of Mnajdra (Gray, 2018).

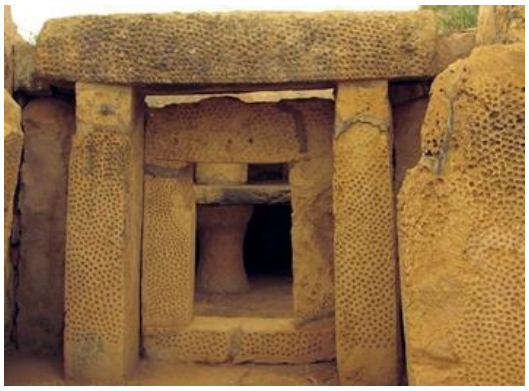

Figure 4: Stone pillar with rows of dots (Holland, 2018) .

3. Field tests and a method for the verification of the numerical model

The measurements of the experimental investigations, which were conducted by ambient vibration monitors, were plotted as a spectral ratio of the horizontal and vertical components (H/V) of the ambient vibration noise from each station recorded. First, the Fourier spectra of the three components (east-west, north-south and vertical) were calculated from the recorded ambient vibration noise which was recording the 3-axial movement (N-S component, E-W component and up-down component) of the structure under ambient vibration. Then, the two horizontal components, east-west and north-south are averaged and divided by the vertical Fourier spectra which results in a H/V curve as a function of frequency (Ullah and Prado, 2016, Layadi et al., 2018). This technique is regarded as one of the fastest and quickest way for investigating the mechanical properties of a structure on site (Ullah and Prado, 2016) since the peak corresponds to the fundamental resonance frequency (Tokimatsu, 1997, Bonnefoy-Claudet et al., 2006). It is noted that in the given framework, no excitation machine was used.

Two ambient vibrator monitors (red and yellow) were placed at various positions (Figure 5) of the monument to record the ambient vibration noise of the structure. Results from eight positions were used for this study since they were positioned on the stones of the internal wall of the monument. These positions are namely, M39, Y33, Y34, R12, Y42, Y35, R10 and R11 as presented on Figure 5. After the measurements are obtained, H/V ratio-frequency plots are created and used to verify the geometry, the mechanical boundary conditions and the material properties of the finite element models which have been developed.

This verification is done by comparing the frequency corresponding to the maximum H/V ratio recorded from the experimental investigation to the natural frequency obtained from the

eigenmode finite element analysis. The position of the ambient vibrator monitor on a specific part of the structure was coupled with the mode shape depicting the highest excitation at this region of the structure, in the eigenmode analysis. The frequency obtained from this mode shape was compared to the corresponding experimental frequency. The H/V ratio-frequency graphs obtained from the experimental investigation, are presented in Figures 6 - 13.

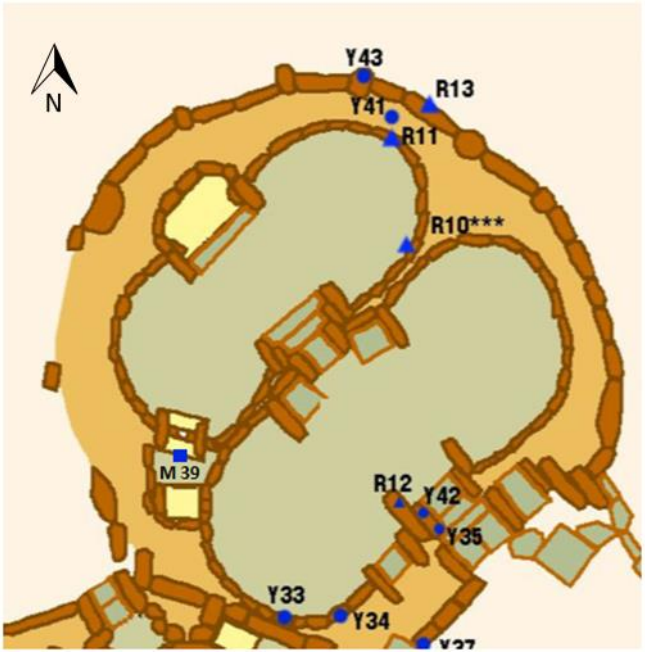

Figure 5: Plan drawing of the middle temple showing the positions where the ambient vibrator monitors were placed on the temple.

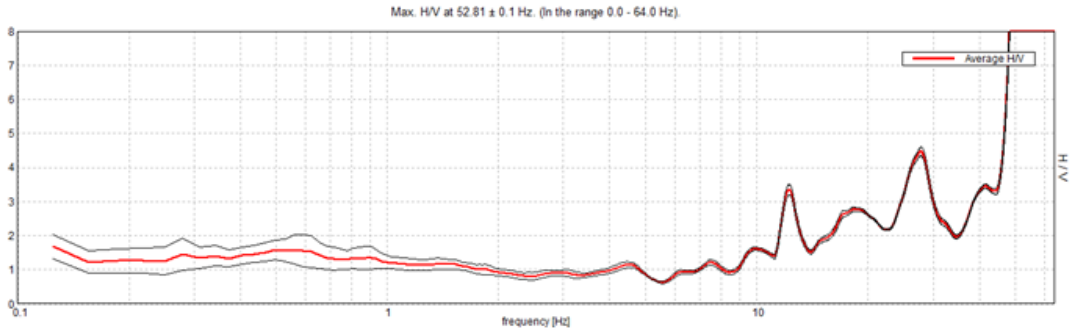

Figure 6: H/V ratio-frequency graph from position Y34 with maximum H/V at 52.81 Hz.

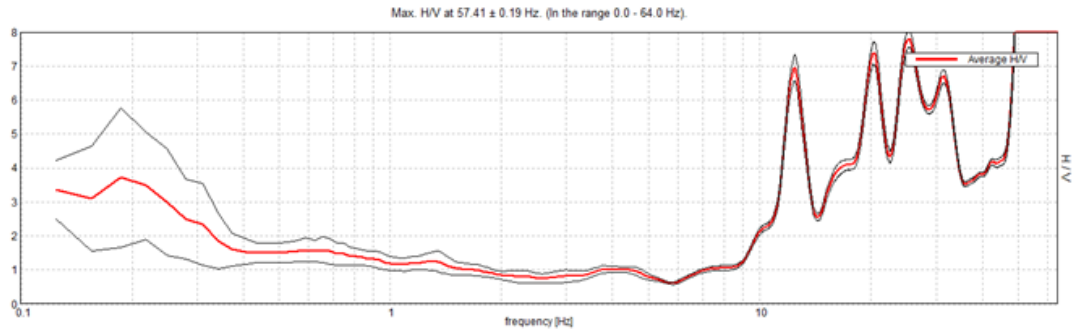

Figure 7: H/V ratio-frequency graph from position Y33 with maximum H/V at 57.41 Hz.

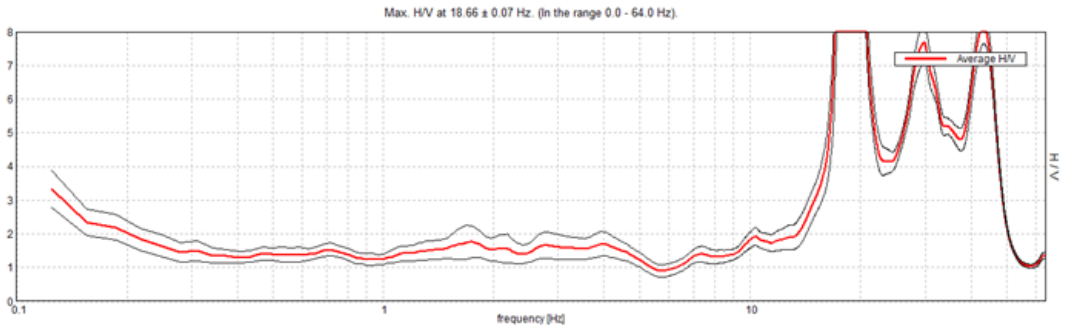

Figure 8: H/V ratio-frequency graph from position R12 with maximum H/V at 18.66 Hz.

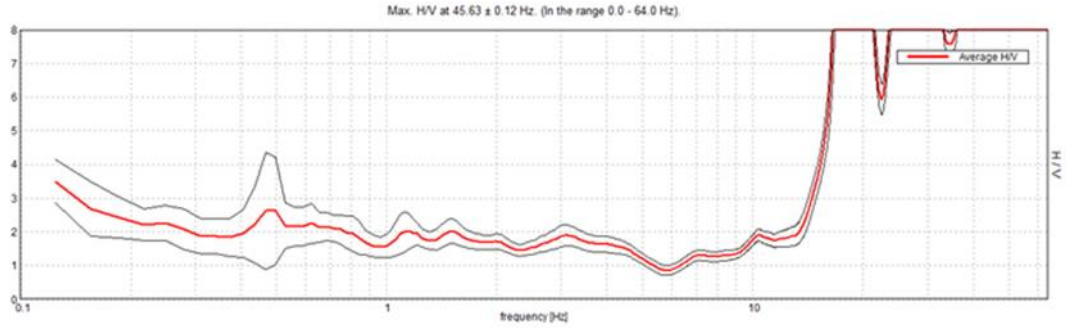

Figure 9: H/V ratio-frequency graph from position Y42 with maximum H/V at 45.63 Hz.

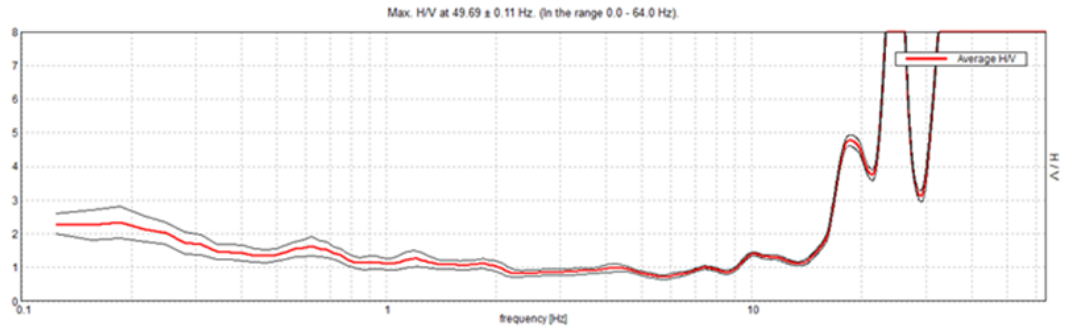

Figure 10: H/V ratio-frequency graph from position Y35 with maximum H/V at 49.69 Hz.

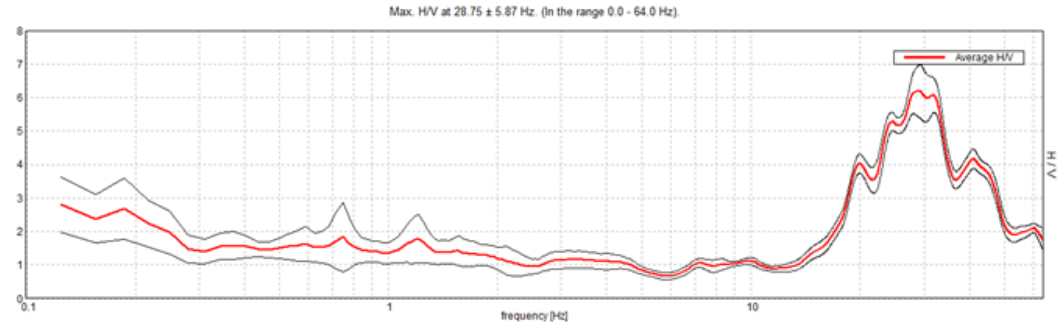

Figure 11: H/V ratio-frequency graph from position R10 with maximum H/V at 28.75 Hz.

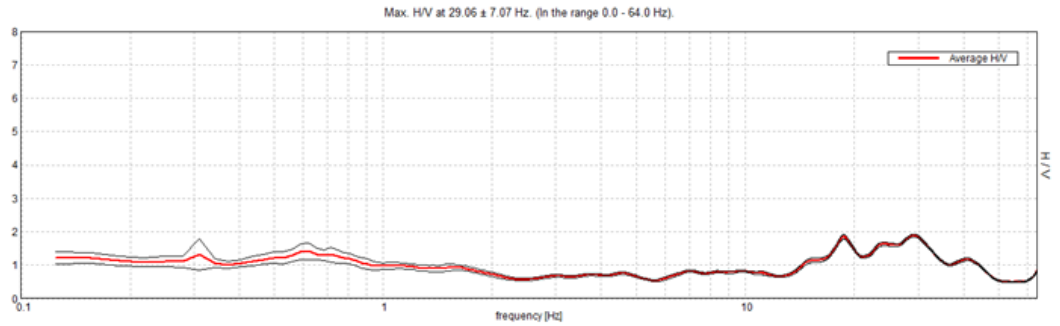

Figure 12: H/V ratio-frequency graph from position R11 with maximum H/V at 29.06 Hz.

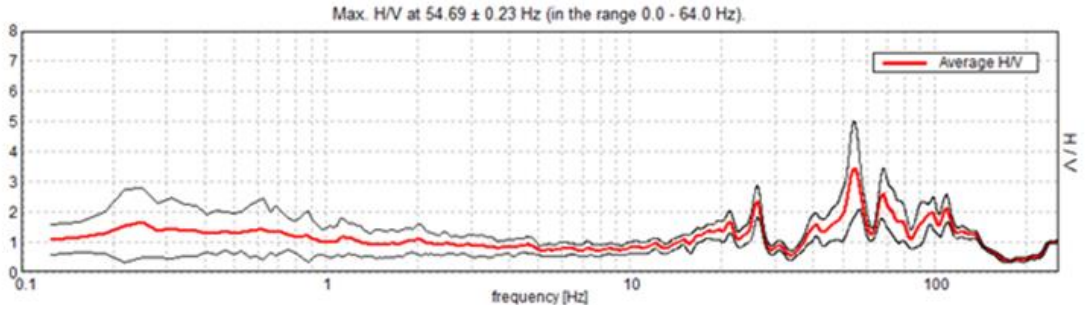

Figure 13: H/V ratio-frequency graph from position M39 with maximum H/V at 54.69 Hz.

4.The computational mechanics experiments

4.1 General description of the model

In modelling the middle temple of Mnajdra, a cloud of points was collected from situ using a radar-laser scanner from which a 3D geometry was created on AutoCAD. The geometry created was exported as a SAT file and was inputted on Abaqus 6.12-3 (Hibbitt et al., 2012) for the creation of the finite element model. The applied mechanical boundary conditions include fixed supports at the bottom of the megaliths.

The model created on Abaqus consists of 123 536 three-dimensional finite elements, Figure 14. Figure 15 shows a closer view of the mesh density of the model. The finite elements are 8-node solid elements (hexahedrons) with three displacement degrees of freedom at each node.

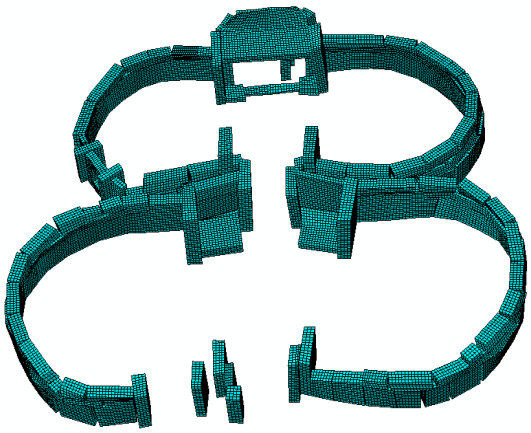

Figure 14: Mesh of the finite element model showing the inner walls and spaces of the middle temple.

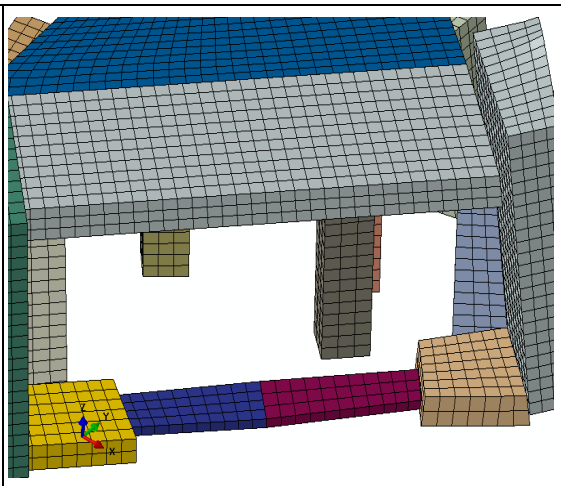

Figure 15: Closer view of the of the model showing the mesh profile of the stones.

4.2 Eigenmode analysis

Comparison between experimental data and eigenmode analysis was carried out in order to verify the developed finite element models. This was achieved by creating several models with different material properties (Young's modulus and density) and comparing their natural frequencies and mode shapes to those obtained from the experimental investigation. For the interface between the stones, a tie-linear constraint or a frictional contact law has been adopted. For the frictional contact law, the following two options are applied, regarding the behaviour of interfaces in the normal direction: separation allowed or separation not allowed. It is pointed out that the loading sequence, which permits the implementation of unilateral contact conditions within linear eigenvalue analysis, initially considers the self-weight of the structure, where the unilateral frictional contact is active, and then the eigenvalue analysis, where the contact conditions remain constant.

Ambient vibrator monitors were placed by researchers from University of Malta in various positions along the monument to obtain the natural frequency of the structure, Figure 5. The measurements obtained from those positions, were used to compare the natural frequencies from the experimental data and the finite element analysis. These positions were chosen since the ambient vibrator monitors were placed in contact with the internal wall of the temple during data collection and the internal wall was modelled on Abaqus as shown on Figure 14. The Lanczos method (Paige, 1972, Lanczos, 1950) was used to solve the eigenmode problem since this method is considered to be adequate for large-scale structures (Stavroulaki et al., 2018).

4.3 Nonlinear static and dynamic analysis

After the developed numerical models have been verified, more numerical simulations are considered to further evaluate the capacity of the monument to resist different load cases. In

particular, first the effects of differential support settlements and backfill are investigated within nonlinear static finite element analysis. The settlement of supports may occur due to faults movement named Hyblean Plateau and Maghrebian Thrust Front (Gardiner et al., 1995), which are present in the region, or weakening of the foundations of the structure due to heavy storms (Cassar, 1988). Then, the performance of the structure is tested within nonlinear time history analysis and an old ground motion loading from a past seismic event.

To simulate the contact conditions between each stone, principles taken from contact mechanics have been adopted. Let u be the single degree of freedom of the system, g be the initial opening and t^n be the corresponding contact pressure in case contact occur, Figure 16. The basic unilateral contact law is described by the following set of inequalities (1), (2) and by the complementarity relation (3) (Panagiotopoulos, 1985, Drosopoulos et al., 2006). Inequality (1) represents the non-penetration relation between the stones, while relation (2) implements the requirement that only compressive stresses (contact pressures) are allowed. This is a logical assumption for the specific structure, since no mortar has been identified between the stones. Equation (3) is the complementarity relation stating that either separation with zero contact stress occurs or contact is realized between the stones, with possibly non-zero compressive stress. For a discretized structure these relations are written for every point of a unilateral boundary or interface. In the following equations, u is the single degree of freedom shown in Figure 16 and g represents the initial opening between the contacting bodies.

$$h = u - g \leq 0 \Longrightarrow h \leq 0 \qquad (1)$$

$$-t^n \geq 0 \qquad (2)$$

$$t^n(u - g) = 0 \qquad (3)$$

The behaviour in the tangential direction between the stone interfaces, is defined by a static version of the Coulomb friction model. Two contacting surfaces start sliding when the shear stress in the interface reaches a critical value equal to:

$$t^t = \tau_{cr} = \pm\mu|t^n| \qquad (4)$$

where t^t and t^n are the shear stress and the contact pressure at a given point of the contacting surfaces respectively and μ is the friction coefficient. There are two possible directions of sliding along an interface, so t^t can be positive or negative depending on that direction. Furthermore, there is no sliding if $|t^t| < \mu|t^n|$ (stick conditions). The sliding rule can be summarized by the following relations, where u_t is the displacement (sliding) in the tangential direction of an interface:

$$|t^t| < \mu|t^n| \longrightarrow u_t = 0 \ (no\ sliding) \qquad (5a)$$

$$t^t = \mu|t^n| \longrightarrow u_t \geq 0 \ (sliding\ in\ one\ diretion) \qquad (5b)$$

$$t^t = -\mu|t^n| \longrightarrow u_t \leq 0 \ (sliding\ in\ the\ opposite\ direction) \qquad (5c)$$

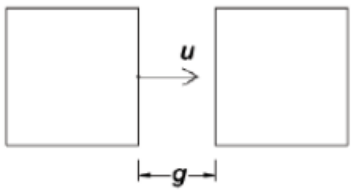

Figure 16: Schematic drawing showing the contact conditions applied on each stone based on contact mechanics

The unilateral contact-friction problem is strongly nonlinear, and the nonlinearity is restricted to the interfaces between the stones. In particular, the nonlinearity is caused by the opening–closure and sticking–slipping along these interfaces. Consequently, the equations of equilibrium are nonlinear even if the material obeys a linear elastic law or a small displacement assumption is made, which is the case in the present work. The contact constraint is enforced with Lagrange multipliers operating the contact pressures. The penalty method is used for the simulation of the frictional phenomena. The overall nonlinear problem is solved within the framework of the Newton-Raphson incremental-iterative procedure.

After the nonlinear static analysis, a dynamic analysis study is performed, in the framework of nonlinear time history analysis. The monument is subjected to a past earthquake which took place in Southern part of Italy (Irpinia) in 1980. It should be mentioned that Malta is also located south of Italy. Due to this earthquake, more than 2000 people were killed in an isoseismic area VII of about 100 km in length (Bernard and Zollo, 1989). The magnitude of this earthquake was 6.69, the accelerometer distance from the epicentre was equal to 30.35 km and the peak ground acceleration (g) equal to 0.29. The ground motion of the seismic event, given in ground acceleration-time diagrams, are given in Figures 17 - 19 for the three dimensions (Berkley, 2018). This data is imported in the numerical model to simulate the effects of the ground motion of this event, on the structural response of the structure. This earthquake was used since it was located in the broader area of the island of Malta, taking place on the southern region of Italy, and was among the more severe seismic events during the last years. However, no recorded structural damage was uncovered on the monuments.

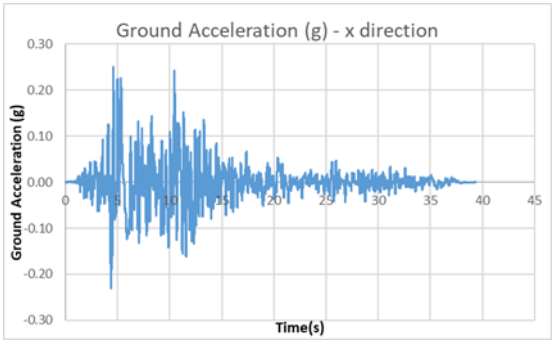

Figure 17: X-direction acceleration-time graph from Irpinia earthquake in Italy,1980.

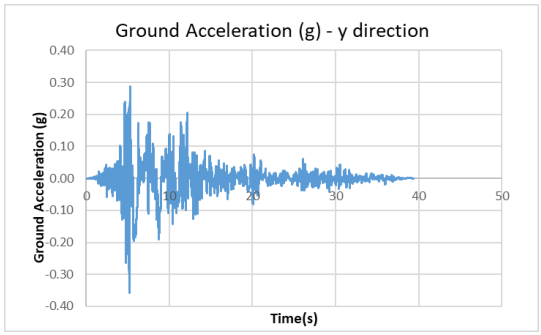

Figure 18: Y-direction acceleration-time graph from Irpinia earthquake in Italy,1980.

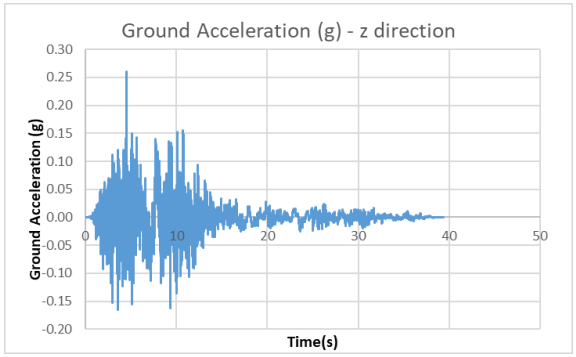

Figure 19: Z-direction acceleration-time graph from Irpinia earthquake in Italy,1980.

5. Results and discussions

5.1 Comparison between experimental output and numerical eigenmodal analysis

In order to verify the finite element model, and properly estimate the material properties of the structure, a comparison between the experimental output data and numerical eigenmode analysis is considered. A series of numerical eigenmode simulations have been carried out in order to undertake a parametric sensitivity analysis of the mechanical properties and contact conditions between the stones.

5.1.1 Geometry and mechanical material properties

The first parametric analysis is conducted to investigate the sensitivity of the mechanical properties on the numerical models. The different material properties adopted are listed in Table 1. The interface conditions between the stones are considered to be the tie-constraint. This is linear elasticity constraint, permitting no opening or sliding between the interfaces.

Table 1: Mechanical properties for the material used for the parametric analysis

Material	Young's modulus, E (GPa)	density (kg/m^3)	Poisson's ratio
M1[1]	22	2800	0.22
M2[1]	20	2628	0.22
M3	6	2300[2]	0.22[1]
M4	5.5	2300[2]	0.22[1]
M5	5	2300[2]	0.22[1]
M6	4.5	2300[2]	0.22[1]
M7	4	2300[2]	0.22[1]

References: [1](Cassar et al., 2017), [2](Cassar, 2010)

From the results of the eigenmode analysis, it can be shown that different parts of the structure are activated at different mode shapes (Figures 20 - 32). The mode shapes were found to be relatively similar for the different models created, however significant differences were obtained for the eigenfrequencies.

The figures below show the positions of the ambient vibration equipment together with the corresponding mode shapes which were identified in the numerical model. Both the experimentally and the numerically obtained frequencies were recorded. The model which depicted the closer comparison to the values found on site is the one with Young's modulus of 4 GPa and density of 2300 kg/m^3. This model is referred to as material, M7 in Table 1. Therefore, results from the numerical model M7 and the positions of the ambient vibration equipment are presented in Figures 20-32.

Figure 20: Position Y33 of yellow ambient vibration monitor with maximum frequency of 57.41 Hz.

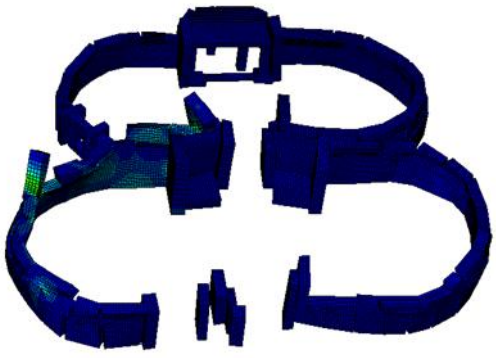

Figure 21: The mode shape with frequency of 52.63 Hz corresponding to Y33.

Figure 22: Position Y34 of yellow ambient vibration monitor with maximum frequency of 52.81 Hz.

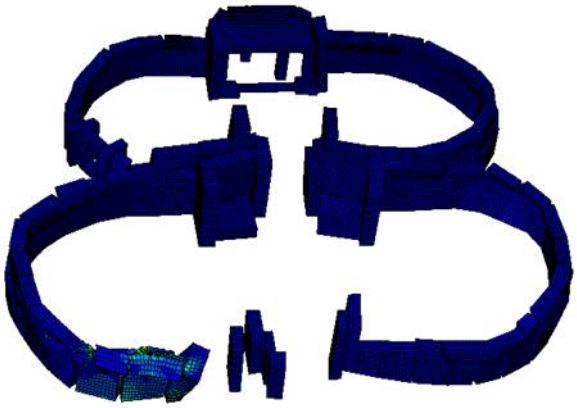

Figure 23: The mode shape with frequency of 57.36 Hz corresponding to Y34.

Figure 24: Positions R12 and Y42 of red and yellow ambient vibration monitor respectively with maximum frequency of 18.66 Hz and 45.63 Hz respectively.

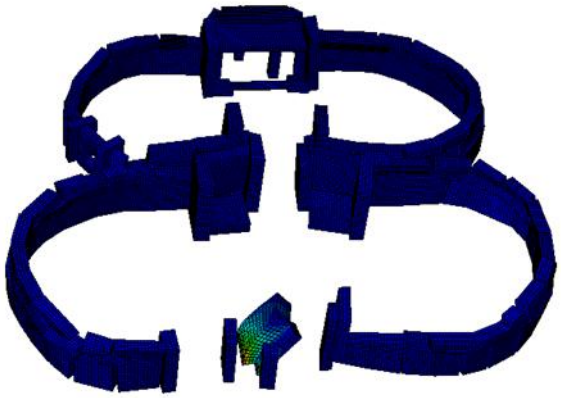

Figure 25: The mode shape with frequency of 51.90 Hz corresponding to R12 and Y42.

Figure 26: Position Y35 of yellow ambient vibration monitor with maximum frequency of 49.69 Hz.

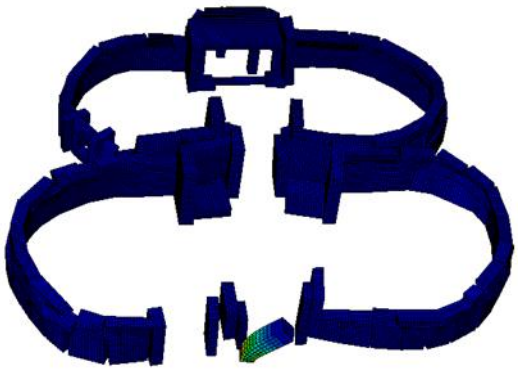

Figure 27: The mode shape with frequency of 41.39 Hz corresponding to Y35.

Figure 28: Position R10 of red ambient vibration monitor with maximum frequency of 28.75 Hz.

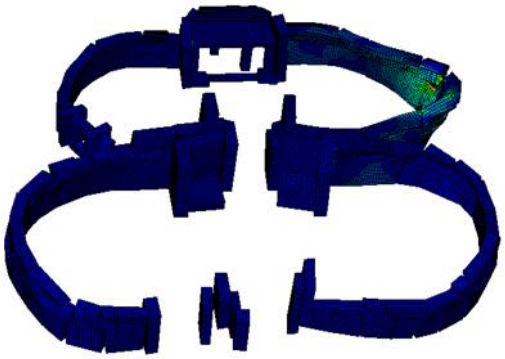

Figure 29: The mode shape with frequency of 42.93 Hz corresponding to R10.

Figure 30: Position R11 of red ambient vibration monitor with maximum frequency of 29.06 Hz.

Figure 31: The mode shape with frequency of 34.71 Hz corresponding to R11.

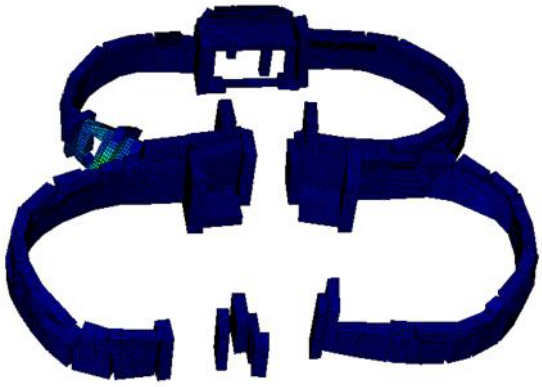

Figure 32: The mode shape with frequency of 54.69 Hz from the model which corresponds to the maximum frequency on 46.39 Hz recorded on position M39 on situ.

5.1.2 Contact conditions between stones

A second parametric analysis was conducted to investigate the sensitivity of the contact conditions between the stones, which are considered to become active when the self-weight is applied, before the numerical eigenmode step. The different numerical models created for this parametric study are listed in Table 2 together with their contact mechanics conditions between the stones. As shown in this Table, different friction coefficients have been considered for the tangential direction of the interfaces, while for the normal direction, opening may or may not allowed. The mechanical properties of the models used in this parametric study are maintained constant with a Young's modulus of 5 GPa and density of 2300 kg/m^3.

Table 2: Contact conditions between the stones of the models used for the parametric analysis.

Model	Friction Coefficient	Opening/ After contact
F1	0.5	Allowed
F2	0.4	Allowed
F3	0.3	Allowed
F4	0.2	Allowed
F5	0.5	Not Allowed
F6	0.4	Not Allowed
F7	0.3	Not allowed

From the results of the parametric study shown in Figure 33, it can be observed that different parts of the structure are activated at different mode shapes, similarly to previous models. The mode shapes and eigenfrequencies were found to be relatively similar when opening is allowed or not, for different friction coefficients (shown in Table 2). This shows that changing the friction coefficient does not significantly affect the subsequent eigenvalue analysis.

In the left side of Figure 33, are depicted the mode shapes when opening is allowed in the interfaces while in the right side are shown the corresponding results when opening is not allowed. It is noted that for positions R12 and Y42, the numerical models did not activate any part of the structure in the area where these vibration monitors are located, when both opening in the interfaces is allowed and not allowed. The same comment applies to the position Y35, for the model where opening is allowed. Figure 33 shows that for some positions of the vibration monitor, different eigenfrequencies and/or different mode shapes are obtained. This indicates that the contact conditions between the megalithic stones may significantly influence the eigenvalue response of the system.

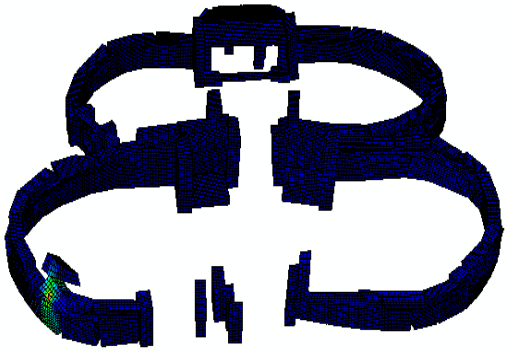 a (left)	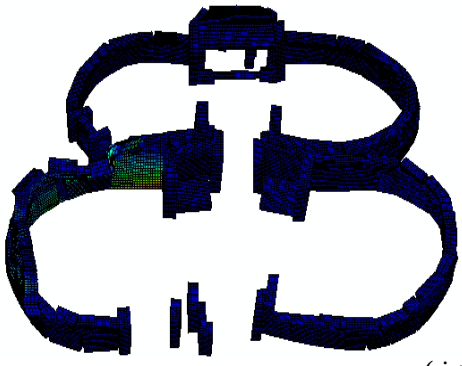 a (right)
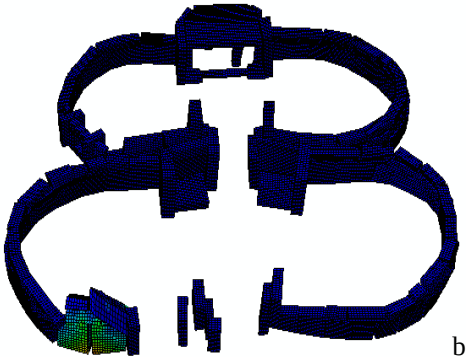 b (left)	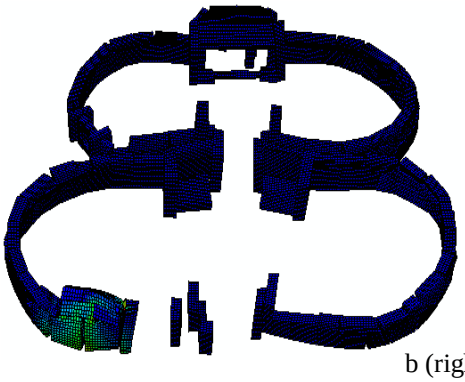 b (right)
No activation on this position from the eigenvalue analysis	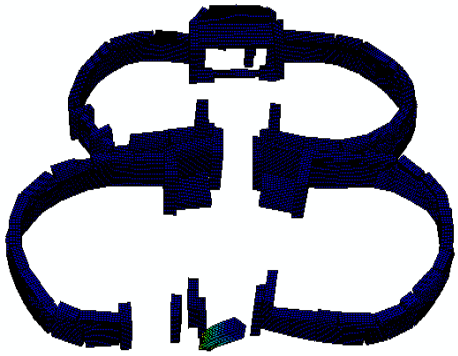 c (right)
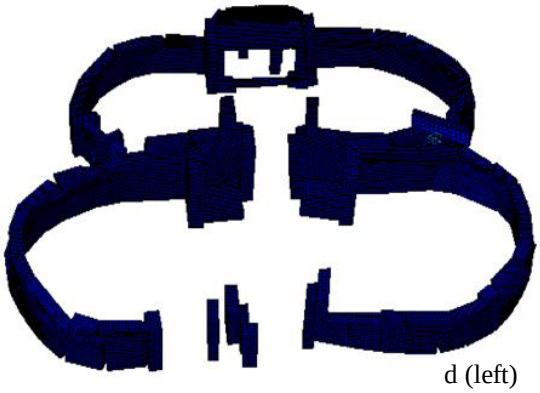 d (left)	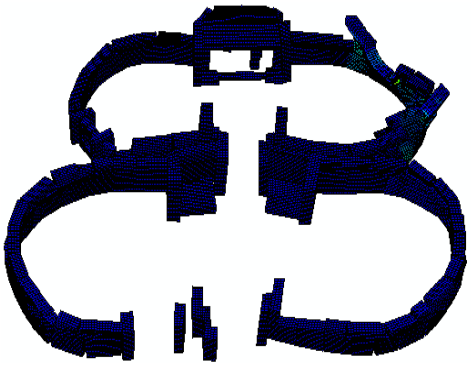 d (right)

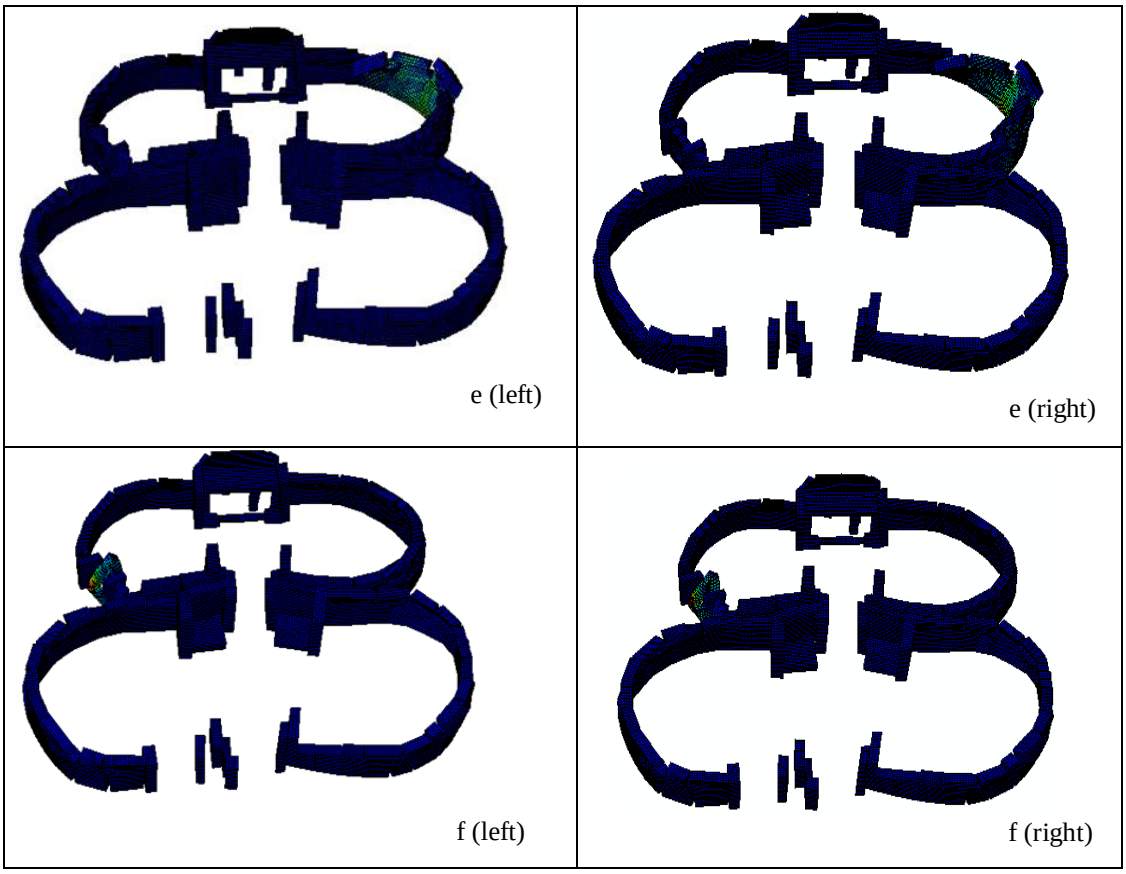

Figure 33: Mode shapes when opening in the interface during self-weight loading is allowed (left) and not allowed (right) with (a) frequency 19.10 Hz (left) and 36.64 Hz (right) corresponding to Y33, (b) frequency 32.50 Hz (left) and 35.31 Hz (right) corresponding to Y34 (c) frequency 46.23 Hz (right) corresponding to Y35 (no proper activation from the model where opening is allowed) (d) frequency 16.55 Hz (left) and 40.40 Hz (right) corresponding to R10, (e) frequency 28.10 Hz (left) and 31.79 Hz (right) corresponding to R11, (f) frequency 35.90 Hz (left) and 36.64 Hz (right) corresponding to M39.

Results from the full parametric eigenmode analysis are plotted on the graph shown in Figure 34. The positions of the ambient vibrator monitors which are shown in Figure 5 are represented by the numbers 1 - 8 on the x-axis of the plot in Figure 33 in the order: Y33, Y34, R12, Y42, Y35, R10, R11 and M39 respectively**.**

Comparison between the experimental and numerical frequency values, shows that a value of Young's modulus used in finite element analysis equal to 4 GPa closely resembles the field tests. Two important deviations are mainly observed, for points 3 and 6 (R12 and R10, respectively). This deviation could be attributed to potential issues during the experimental measurements, or the fact that weak soil is not simulated in this work.

Since a satisfactory comparison is received from 6 out of 8 points, the goal of this investigation, to verify material properties and the geometry of the numerical model, has been achieved.

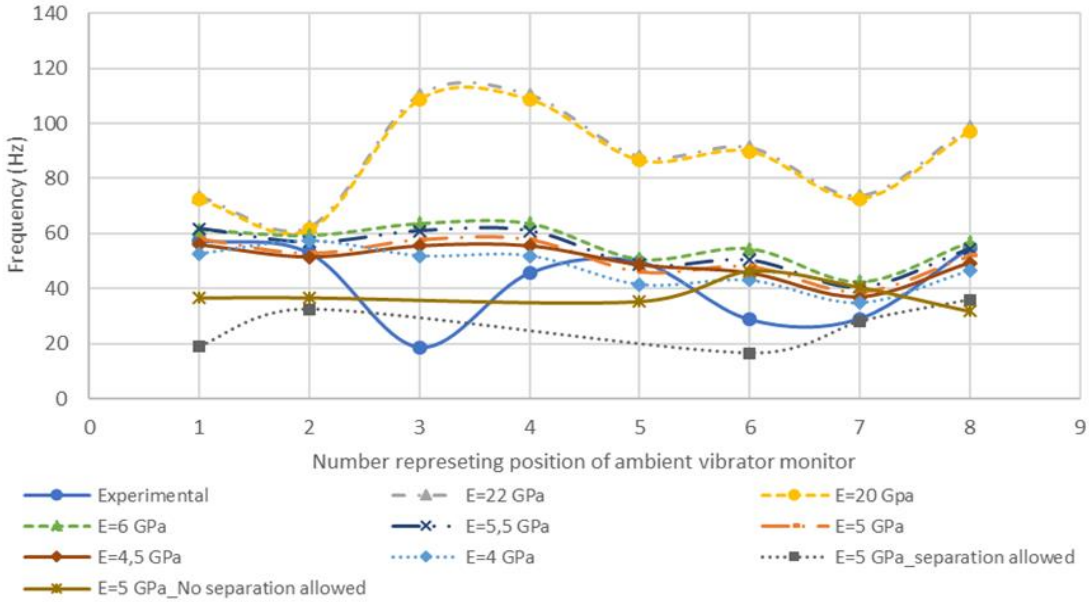

Figure 34: Parametric graph showing the comparison between numerical and experimental output for the natural frequencies of the structure.

5.2 Nonlinear static analysis

The effects of differential settlement of supports and increased pressure due to backfill are investigated by using a nonlinear static structural analysis. The settlement of supports may occur due to a fault movement or weakening of the foundations of the structure following heavy storms. In the models created for the investigation of differential settlement, the settlement was considered vertically in certain regions of the supports while the other regions without settlement were fixed in all three direction, Figure 35.

Increase in pressure due to the backfill may take place due to heavy rainfall. This particular phenomenon, which was observed in 1995, resulted in the collapse of some stones in region R5 of M7, highlighted in Figure 35 (Torpiano, 1995). Other effects, like strong winds, blasting operations from close-by limestone quarries and the lack of water drainage system also contributed to the collapse of the wall in 1995, however research by Torpiano (1995) concluded, that heavy rainfall was the major cause of collapse. Figure 36 shows the loading from the backfill pressure on this particular part of the wall.

Following the collapse of the wall of the monument in 1995, a wall of concrete bricks was constructed behind the original megalithic wall to prevent the development of excessive pressure on the original megalithic wall (Torpiano, 1995). Hence, the effects of backfill on the models of differential settlement were not taken into consideration.

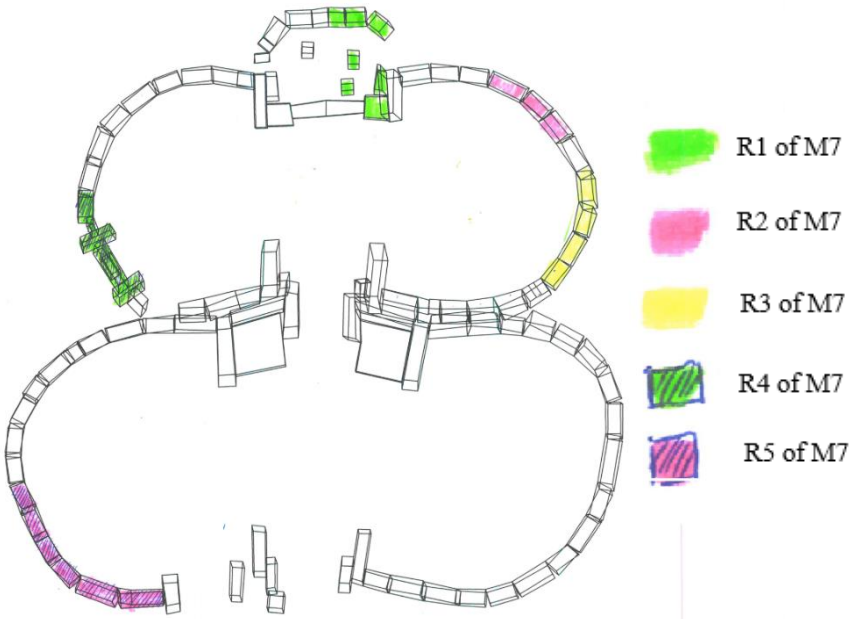

Figure 35: Plan view showing the supports which were settled.

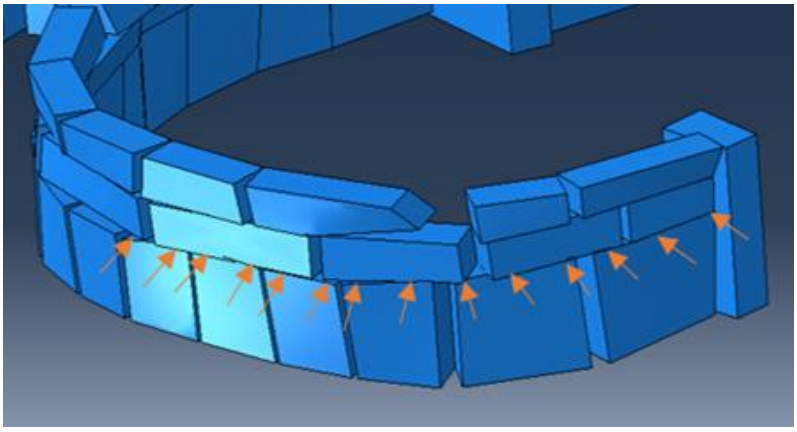

Figure 36: Direction of displacement loading simulating the backfill pressure (in region R5 of Figure 33) in Model D6.

Two steps have been considered in the numerical model. The first step is a dynamic implicit analysis in a quasi-static framework, introducing a gravity load (self-weight) of 9.81 m/s^2. It was found, that due to the extensive number of unilateral contact-friction interfaces, which are used to simulate the contact conditions between each stone, numerical singularities did not allow the model to reach convergence, in case a static analysis was used in the first step. This numerical instability was attributed to multiple micro openings/closures between stone interfaces, resulting in unstable stiffness matrices. To overcome this problem, the mentioned dynamic implicit analysis, in a quasi-static framework, was used. This introduced the mass stiffness in the equilibrium equations, resulting in more stable stiffness matrix.

The second step is a general static analysis where the displacement of supports and stones is applied depending whether support settlement or backfill effects are investigated, respectively. The mechanical properties used are those validated from the eigenmode analysis:

Young's modulus, E = 4 GPa

Density, ρ =2300 kg/m^3

Poisson ratio, ν = 0.22

When support settlement is considered, a vertical displacement of 10 cm is applied to the bottom part of the bottom stones, as a uniform (regarding space) displacement loading. This uniform displacement, is linearly applied, taking values from zero to the maximum one (10 cm). However, when failure due to overturning takes place, analysis is terminated, and the maximum value is not reached. To consider the effects of the backfill pressure at region R5 of M7 (Figure 35), a horizontal displacement of 10cm is applied perpendicular to the face of the stones, at the top edge of the bottom stones as shown in Figure 36, while the supports are kept fixed in all directions. The interface between the stones is frictional with a selected friction coefficient factor of 0.3 which is obtained from research of similar structures (Byerlee, 1978).

Damage of the monument due to support settlements, which includes overturning of stones and opening/closure of gaps between the stone interfaces can be observed in Figures 37 to 41.

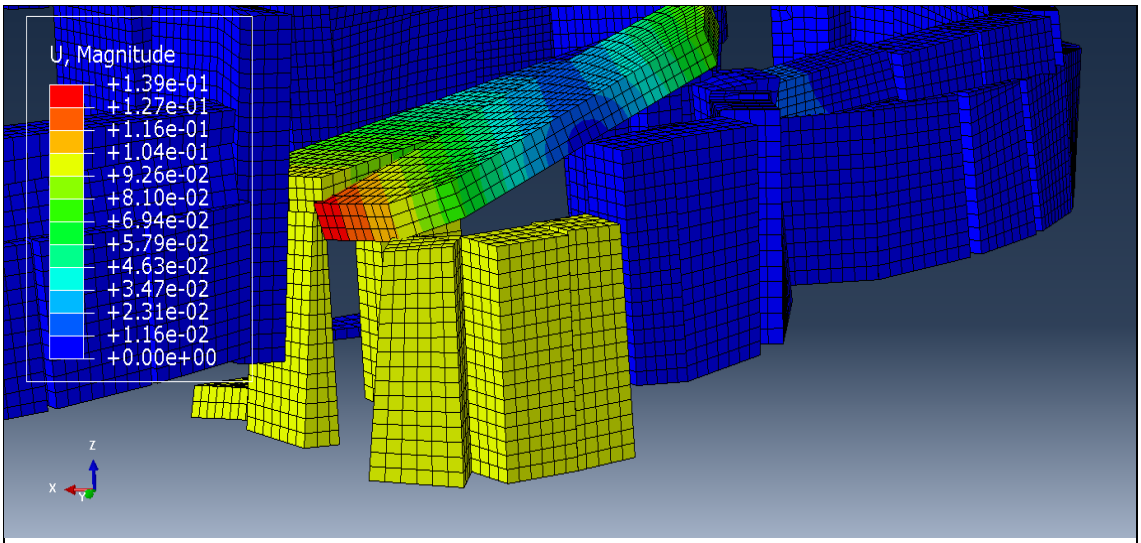

Figure 37: Deformation of monument due to settlement of supports in region R1 of M7.

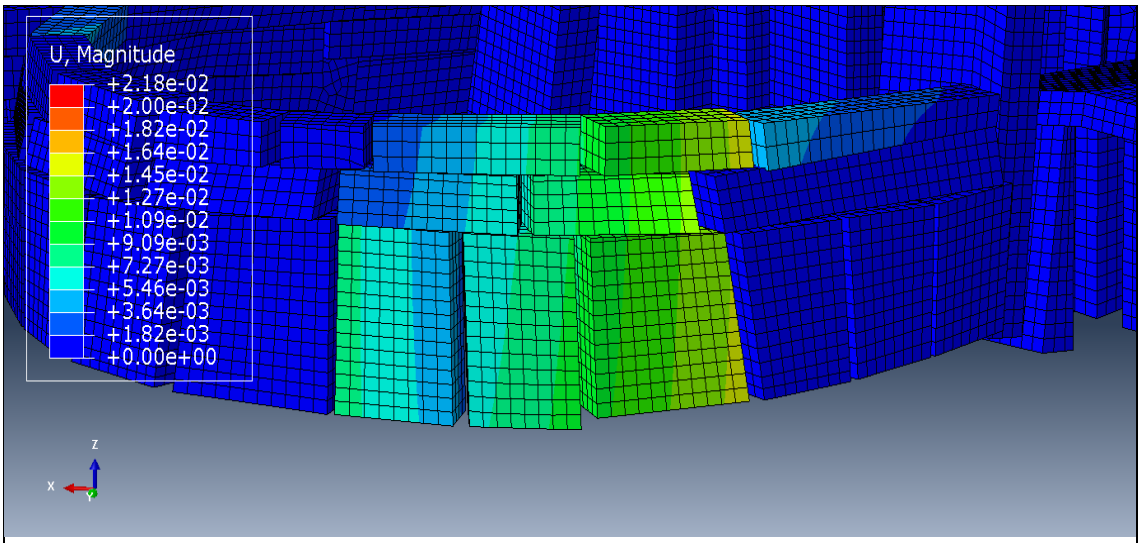

Figure 38: Deformation of monument due to settlement of supports in region R2 of M7.

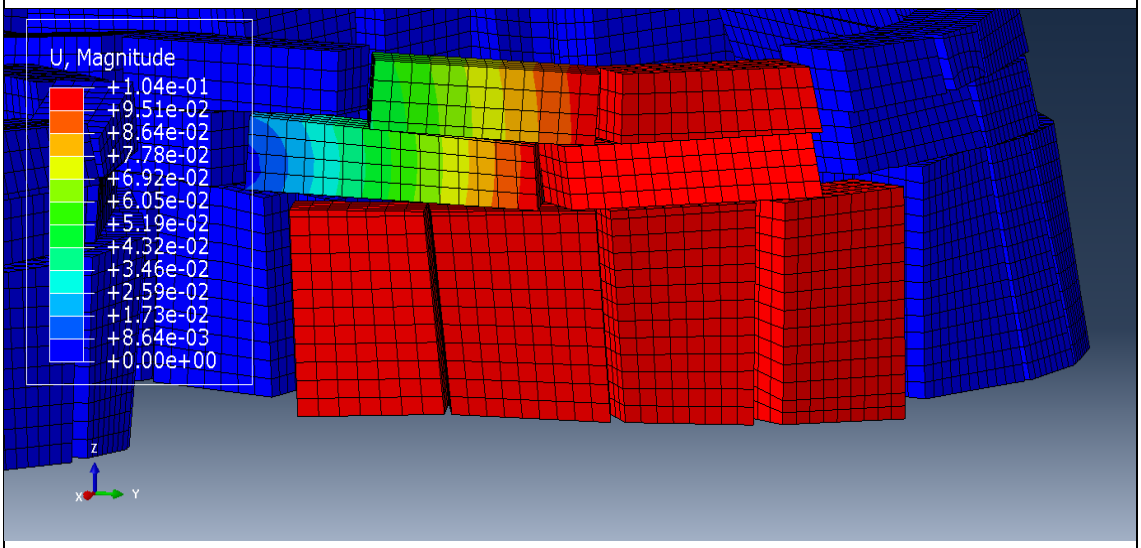

Figure 39: Deformation of monument due to settlement of supports in region R3 of M7.

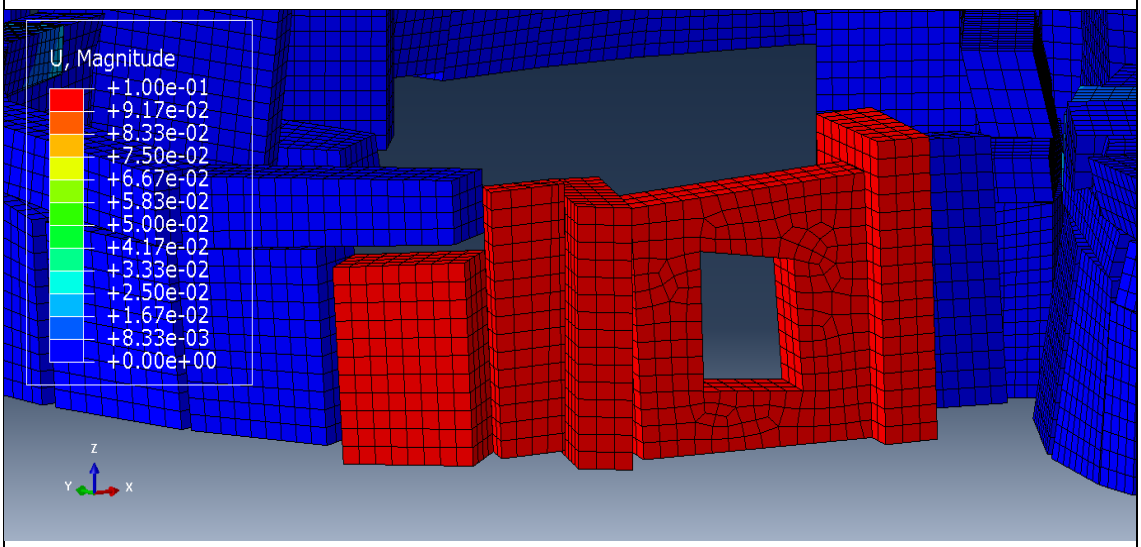

Figure 40: Deformation of monument due to settlement of supports in region R4 of M7.

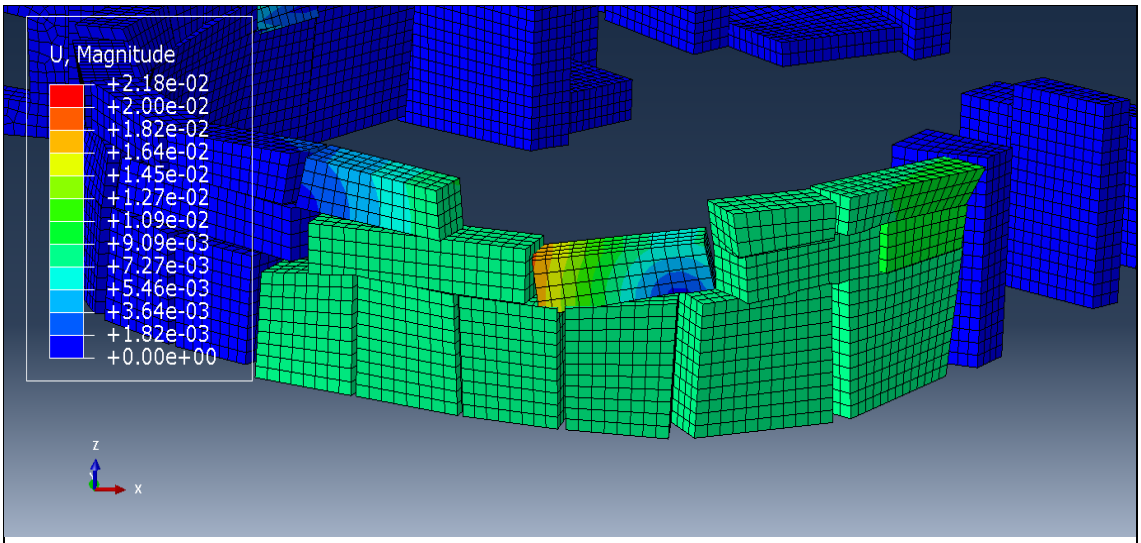

Figure 41: Deformation of monument due to settlement of supports in region R5 of M7.

From these results it can be concluded that differential settlement can proved to be a serious threat for the structural integrity of the monument. The gaps between the stone interfaces tend to open-up and/or widen and this significantly increases the possibility of the stones to dislodge from their stable positions and overturn. In the model R1 of M7 (Figure 37), the horizontal 'roof' stone slab shows the most severe structural failure as compared to the other models with differential settlement. From the numerical simulations, it was also observed that the position of the centre of mass of the stone is important for the structural behaviour. When a stone lies under a stable, unsettled stone (Figure 39-41), the stability of the stone may not be initially affected, since the underlying (stable) stone will serve as its support structure. However, this leaves some of the stones to hang over which significantly increases the risk for overturning (Figure 40).

Another conclusion is that the movement of one stone can cause a ripple reaction which causes stones in the surrounding region to be destabilized. This is more pronounce in the model D6 (Figures 36 and 43), where a horizontal displacement load of 10cm was applied perpendicular to the face of the stones at the top edges of the bottom stones. The results show some of the surrounding stones to be dislodged into the opposite direction of the load applied (Figure 43). A similar damage pattern, depicting stones dislodged from their stable positions and overturning, was obtained after the actual event took place in 1995, Figure 42.

Figure 42: Collapsed wall from first apse of Middle Temple (Torpiano, 1995).

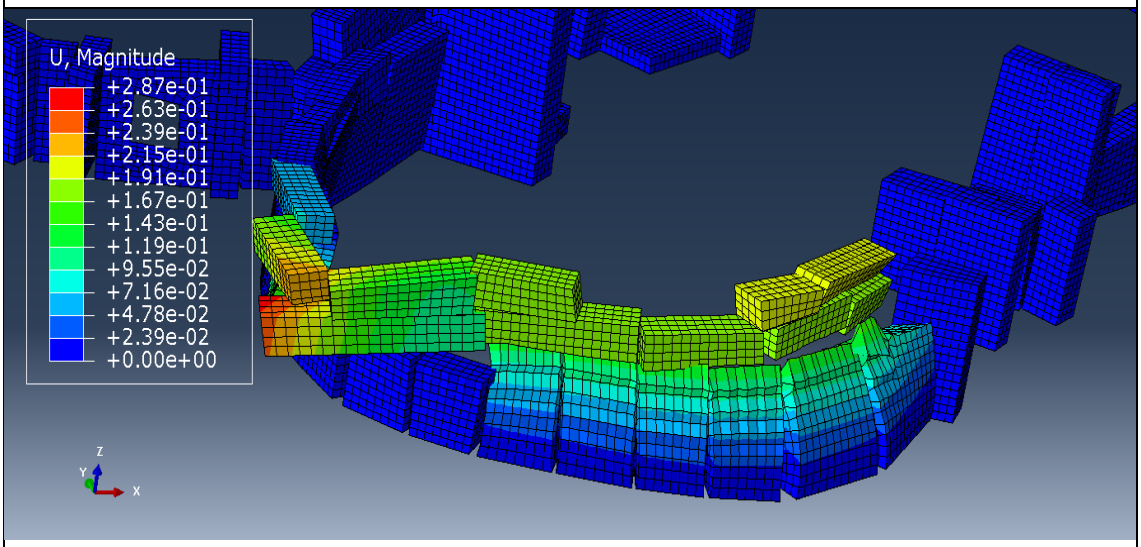

Figure 43: Deformation due to backfill pressure in Model D6.

5.3 Nonlinear dynamic-time history analysis

In this analysis, the effects of seismic activities are taken into account in the form of an earthquake with magnitude of 6.69. In this model two load steps have also been considered. The first step introduces the self-weight, while the second is a dynamic analysis step, using moderate dissipation. Moderate dissipation method uses energy dissipation to moderately dissipate energy due to plasticity, viscous damping, or other effects without significantly affecting the accuracy of the solution (Simulia, 2013).

Within the first step, fixed supports are considered while for the second, the acceleration-time diagrams shown in Figures 17 - 19, are applied as amplitudes on the three different directions of the supports, to fully simulate the ground motion due to the earthquake. The results from the model are show in the Figures 44 - 50.

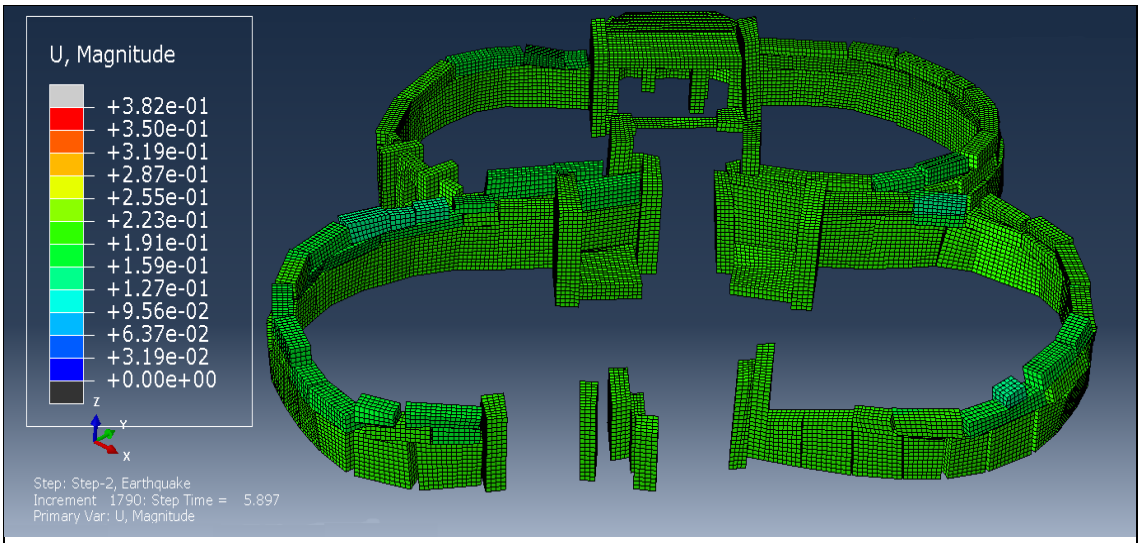

Figure 44: Deformation of monument at 5.9s from the beginning of earthquake, which shows that majority of the structure is deformed by about 22.3cm.

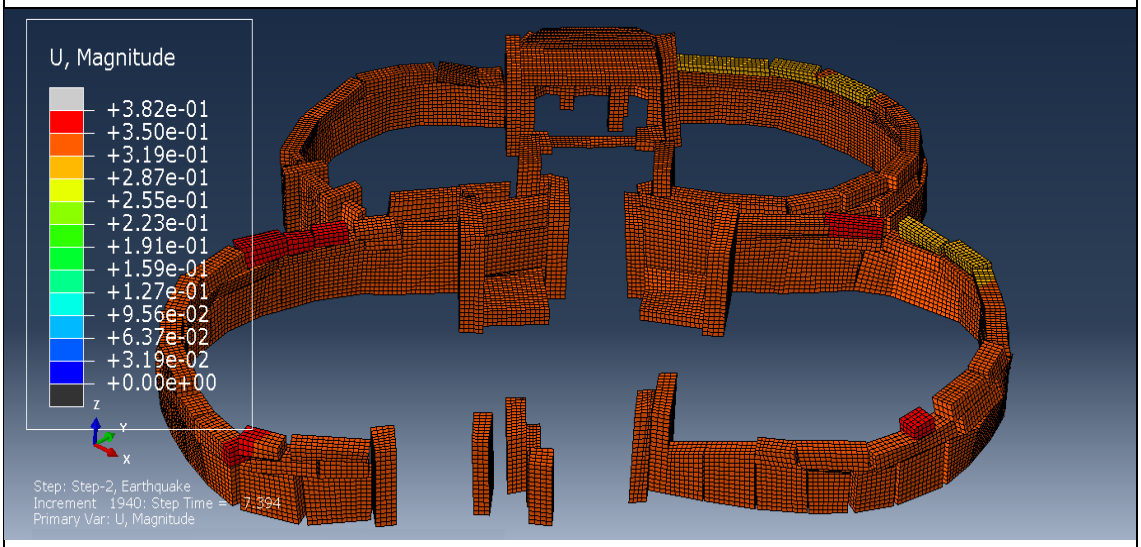

Figure 45: Deformation of monument at 7.4s from the beginning of earthquake, which shows that majority of the structure is deformed by about 31.9cm.

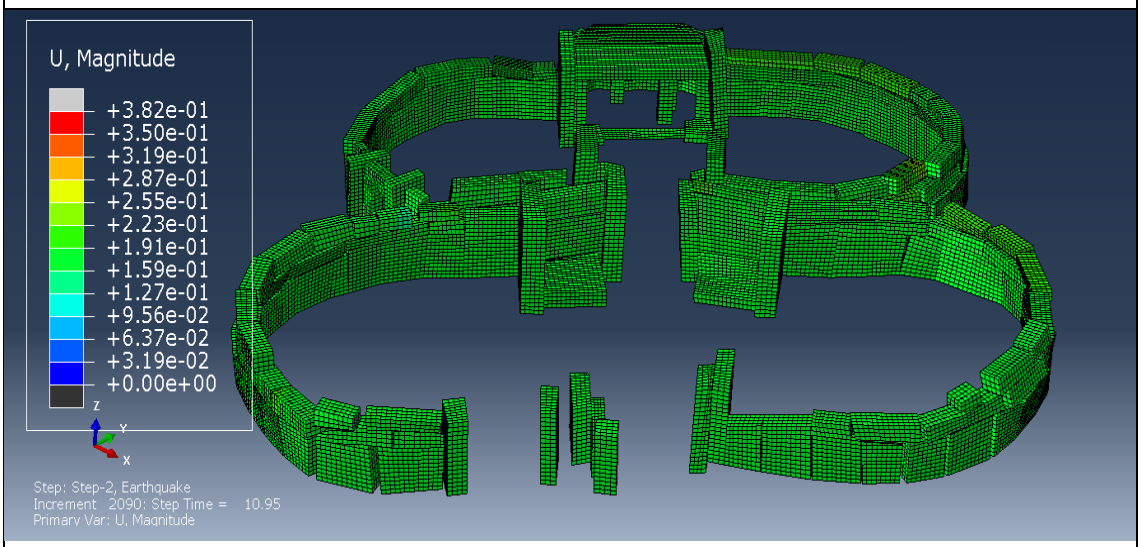

Figure 46: Deformation of monument at 11.0s from the beginning of earthquake, which shows that majority of the structure is deformed by about 19.1cm.

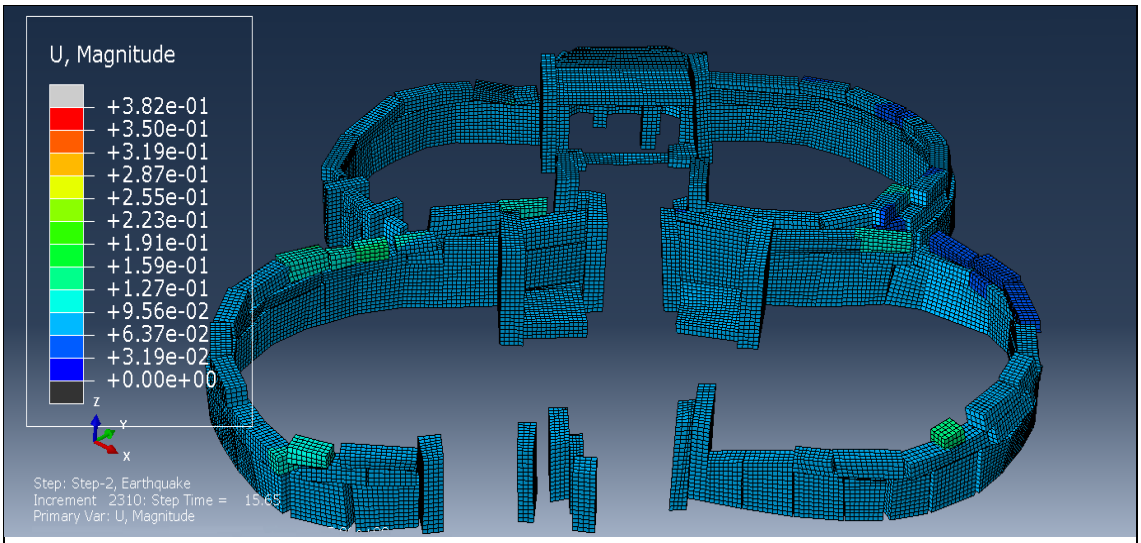

Figure 47: Deformation of monument at 15.7s from the beginning of earthquake, which shows that majority of the structure is deformed by about 6.37cm.

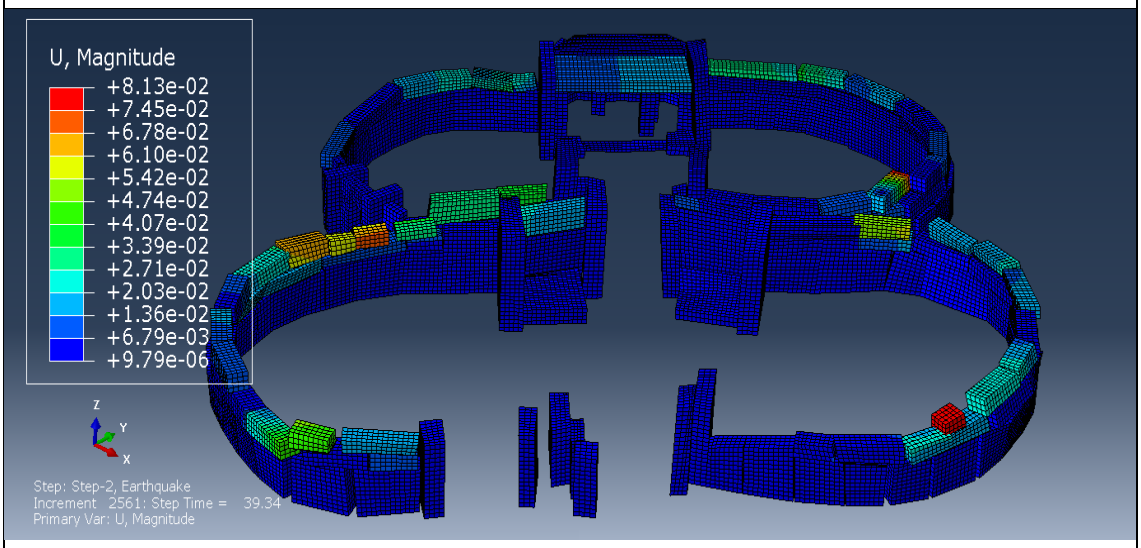

Figure 48: Deformation of monument at the end of the earthquake, at 39.3s, which shows that the majority of the structure is deformed by about 0.001cm.

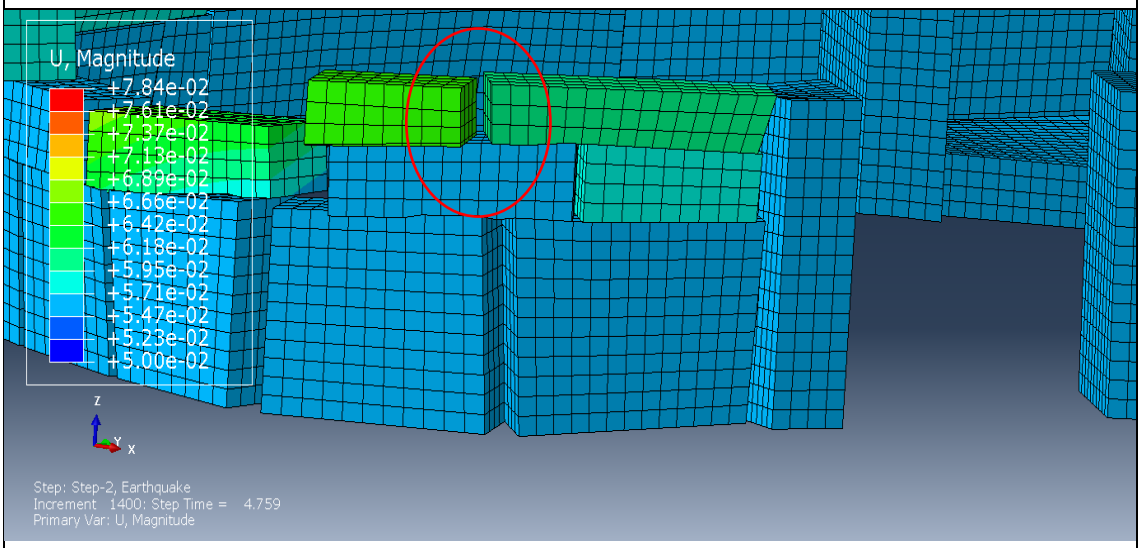

Figure 49: Deformation of monument at 4.8s from the beginning of earthquake, showing opening of contact between stones (circled).

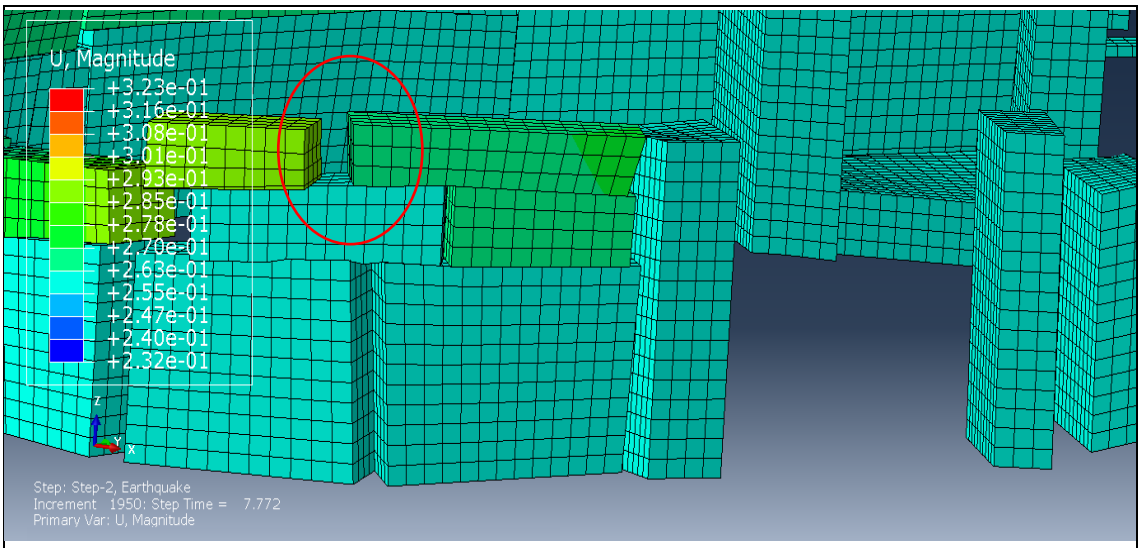

Figure 50: Deformation of monument at 7.8s from the beginning of earthquake, showing opening of contact between stones (circled).

The results from the dynamic analysis show that the structure experiences higher deformation when the acceleration of the ground motion reaches maximum values, while after these peaks are reached, the deformation of the structure is reduced. From the ground motion data (Figure 17 - 19), four peaks can be noticed at about 4.4s, 7.0s, 10.4s and 15s which can trigger higher deformation.

The first maximum deformation experienced by the structure due to the first peak at 4.4s (Figures 17 - 19), is about 22.3cm (Figure 44). This means that it took the monument about 1.5s for it to fully react to this peak in ground motion, since the maximum deformation due to this peak takes place at about 5.9s (Figure 44).

The second maximum deformation experienced by the monument due to the earthquake is approximately 31.9cm (Figure 45), and it's the highest deformation experienced during the course of the earthquake. This takes place at about 7.7s from commence of earthquake. The highest maximum deformation is experienced at this point because the ground motion peaks at about the same time (7s) in all three directions as shown in Figure 17-19, and the state of inertia of the monument was at a relatively higher velocity due to the previous peak since the body was already in motion.

The next maximum peak in ground motion takes place at about 10.4s. This gives a maximum deformation of about 19.1cm (Figure 46), which is reached at approximately 11s. The deformation is smaller compared to the previous deformations even though the ground motion peaks in all three directions. This is due to the fact that the peak of the ground motion is relatively smaller compared to the other peaks. The last peak in ground motion takes place at about 15s, and this gives a deformation of about 6.37cm (Figure 47) which is reached at 15.7s. This deformation

is small compared to the previous deformations because the ground motion peak takes place only on the x- and y-directions, and at this stage, the ground motion peaks are decaying.

At the end of the earthquake, at about 39.4s, most of the stones experience almost zero (about 0.001cm) deformation (Figure 48). However, some of the stones, (top layer stones) were moved (due to sliding) from their initial positions by about 8.13cm without being dislodged. Some gaps between the stones, which had been relatively small or closed (in-contact) before the seismic loading, were opened and/or widen after the dynamic effects (Figures 49 - 50).

As the earthquake progressed, the gaps between the stones increased making the stones more susceptible to dislodging and overturning. This is shown in Figures 49 - 50, where the contact between the stones is opening due to the earthquake.

6. Conclusion

In this study, the structural analysis of the middle temple of Mnajdra is investigated, using experimental research and numerical finite element analysis. Different loading cases have been used to assess the structural response of the structure: differential settlement of supports due to movement of faults and weak soil; displacement of stones due to excessive backfill after heavy rainfall; and seismic activities in the form of an earthquake of magnitude 6.69.

The finite element model used for the structural analysis of the temple was modelled based on in-situ survey of the existing geometry as well as the history of the monument in terms of which are the critical loads that the monument has been subjected to before, or most likely to be subjected in the future. The 3D geometry used for the investigation was created on AutoCAD, using a cloud of points of the temple collected by researchers in Malta. A radar-laser scanner was used to obtain these points. The geometry was then imported on Abaqus finite element commercial package and a finite element model was created, respectively.

To simulate the real contact conditions between the stones, unilateral frictional contact interfaces were used between the stones. The developed model was strongly nonlinear due to these interfaces and the Newton-Raphson incremental – iterative approach was used to solve the numerical problem.

First, the mechanical material properties, geometry and support conditions of the finite element model were verified by comparison of eigenmode analysis and corresponding experimental data. The experimental data was collected using an ambient vibration monitor positioned at various parts of the monument. The comparison between the experimental and numerical model was done by using the natural frequencies obtained from both the site and numerical analysis. From the

comparison, 6 out 8 of the natural frequencies matched closely to the experimental data hence the model was verified.

Secondly, a nonlinear static analysis was carried out using the verified model from the eigenmode analysis. In this analysis, the effects of differential settlement of supports which may be due to the movement of faults and weakening of underlying soil, have been studied. Also, the recreation of the collapse of parts of the monument due to the increase in backfill pressure, following heavy rainfall which took place in 1995, was considered. From this analysis, it can be concluded that:

1. Differential settlement is a major contributor to the damage of the monument since some stones move from their stable position which results in the creation and/or widening of gaps in-between the stones. This can also result in stones dislodging and tipping over. A ripple effect can be experienced by some stones, in the neighbourhood of the stones that settle. This disturbs the dependant stones from their position of inertia which can result in tipping them over.

2. The structural integrity of the monument can be significantly reduced by the increase in backfill pressure due to heavy rainfall. This was one of the major causes of the first apse wall to collapse in 1995. The failure pattern from the numerical model closely matched the damage pattern from the real collapse. From this study, a better understanding of the effects of increase in backfill pressure is achieved. This explains a subsequent intervention, where a new drainage system was built following that event.

Lastly, a nonlinear dynamic analysis was carried out to investigate the structural behaviour of the monument due to seismic action. The unilateral contact-friction interfaces were kept active, to simulate possible opening, sliding and overturning between the stones. The ground motion of a past earthquake event, which took place in the Southern part of Italy (Irpinia) in 1980, was chosen as the main earthquake scenario. The location of this seismic event is relatively close to the monument under investigation. The ground motion was applied as acceleration-time diagrams in three dimensions, at the supports of the structural model. From this analysis, it was shown that gaps between some of the stones may arise and/or widen due to earthquake, which may lead to the stones losing stability. After the dynamic analysis is completed no severe damage or overturning of stones is depicted.

Further research can incorporate a more detailed description of the monument, taking into account all the structural components, such us the backfill pressure around the whole structure. The study may also be applied to the neighbouring temples, to provide a more holistic view for their structural response.

Acknowledgements

Mr. Siphesihle Mpho Motsa has been supported from the National Research Foundation (NRF) (Dr. G.A. Drosopoulos's fund for rated researchers) and TB Davis scholarship.

References

Aguilar, R., Montesinos, M. & Uceda, S. 2017. Mechanical characterization of the structural components of Pre-Columbian earthen monuments: Analysis of bricks and mortar from Huaca de la Luna in Perú. *Case Studies in Construction Materials,* 6**,** 16-28.

Aktaş, Y. D. & Turer, A. 2015. Seismic evaluation and strengthening of nemrut monuments. *Journal of Cultural Heritage,* 16**,** 381-385.

Augusti, G., Ciampoli, M. & Giovenale, P. 2001. Seismic vulnerability of monumental buildings. *Structural Safety,* 23**,** 253-274.

Bayraktar, A., Altunisk, A. C., Sevim, B. & Turker, T. 2007. Modal testing and finite element model calibration of an arch type steel footbridge. *Steel and Composite Structures,* 7**,** 487-502.

Bayraktar, A., Sevim, B., Altunişik, A. C. & Türker, T. 2010. Earthquake analysis of reinorced concrete minarets using ambient vibration test results. *The Structural Design of Tall and Special Buildings,* 19**,** 257-273.

Berkley, P. 2018. *PEER Strong Ground Motion Database* [Online]. Available: https://peer.berkeley.edu/peer-strong-ground-motion-database [Accessed 12 September 2018].

Betti, M. & Galano, L. 2012. Seismic Analysis of Historic Masonry Buildings: The Vicarious Palace in Pescia (Italy). *Buildings,* 2**,** 63.

Betti, M., Galano, L. & Vignoli, A. 2016. Finite Element Modelling for Seismic Assessment of Historic Masonry Buildings. *In:* D'Amico, S. (ed.) *Earthquakes and Their Impact on Society.* Cham: Springer International Publishing.

Betti, M. & Vignoli, A. 2008. Assessment of seismic resistance of a basilica-type church under earthquake loading: Modelling and analysis. *Advances in Engineering Software,* 39**,** 258-283.

Betti, M. & Vignoli, A. 2011. Numerical assessment of the static and seismic behaviour of the basilica of Santa Maria all'Impruneta (Italy). *Construction and Building Materials,* 25**,** 4308-4324.

Bianco, L. 1999. Geocultural activity in seventeenth and eighteenth century Malta. *GeoJournal,* 48**,** 337.

Bianco, L. 2017. Techniques to determine the provenance of limestone used in Neolithic Architecture of Malta. *Romanian Journal of Physics,* 62**,** 901.

Bonnefoy-Claudet, S., Cornou, C., Bard, P.-Y., Cotton, F., Moczo, P., Kristek, J. & Fah, D. 2006. *H/V ratio: A tool for site effects evaluation. Results from 1-D noise simulations*.

Borg, R. P., Galea, P. & d'Amico, S. 2018. Experimental investigation of Mnajdra megalithic monument. Unpublished research: University of Malta.

Byerlee, J. 1978. Friction of rocks. *Rock friction and earthquake prediction.* Springer.

Capecchi, D. & Vestroni, F. Study of dynamic behaviour of an old masonry building. Proceedings of the 1st European Conference on Structural Dynamics, 1991.

Carpinteri, A., Invernizzi, S. & Lacidogna, G. 2005. In situ damage assessment and nonlinear modelling of a historical masonry tower. *Engineering Structures,* 27**,** 387-395.

Casarin, F. & Modena, M. 2006. Structural assessment and seismic vulnerability analysis of the Reggio Emilia Cathedral, Italy. *Proceeding of Structural Analysis of Historical Constructions*.

Cassar, J. 1988. Past stone restoration methods in the Maltese Islands.

Cassar, J. 2002. *Deterioration of the Globigerina Limestone of the Maltese Islands*.

Cassar, J. 2010. The use of limestone in a historic context–the experience of Malta. *Geological Society, London, Special Publications,* 331**,** 13-25.

Cassar, J., Cefai, S., Grima, R. & Stroud, K. 2018. Sheltering archaeological sites in Malta: lessons learnt. *Heritage Science,* 6**,** 36.

Cassar, J., Galea, M., Grima, R., Stroud, K. & Torpiano, A. 2011. Shelters over the Megalithic Temples of Malta: debate, design and implementation. *Environmental Earth Sciences,* 63**,** 1849-1860.

Cassar, J., Torpiano, A., Zammit, T. & Micallef, A. 2017. Proposal for the nomination of Lower Globigerina Limestone of the Maltese Islands as a" Global Heritage Stone Resource". *EPISODES,* 40**,** 221-231.

Cattari, S., Degli Abbati, S., Ferretti, D., Lagomarsino, S., Ottonelli, D. & Tralli, A. 2014. Damage assessment of fortresses after the 2012 Emilia earthquake (Italy). *Bulletin of earthquake engineering,* 12**,** 2333-2365.

Del Piero, G. 1984. Le costruzioni in muratura.: Springer-Verlag, NJ.

Dooms, D., Degrande, G., De Roeck, G. & Reynders, E. 2006. Finite element modelling of a silo based on experimental modal analysis. *Engineering Structures,* 28**,** 532-542.

Drosopoulos, G. A., Stavroulakis, G. E. & Massalas, C. V. 2006. Limit analysis of a single span masonry bridge with unilateral frictional contact interfaces. *Engineering Structures,* 28**,** 1864-1873.

Evans, J. D. 1971. *The prehistoric antiquities of the Maltese islands: a survey*, University of London, Athlone Press.

Fitzner, B., Heinrichs, K. & Volker, M. 1997. Model for salt weathering at Maltese Globigerina Limestones.

Galdies, C. 2011. *The climate of Malta: statistics, trends and analysis 1951–2010.* [Online]. Malta: National Statistics Office. Available: https://nso.gov.mt/en/publicatons/Publications_by_Unit/Documents/B3_Environment_Energy_Transport_Agriculture_Statistics/The_Climate_of_Malta.pdf [Accessed 16 March 2018].

Gardiner, W., Grasso, M. & Sedgeley, D. 1995. Plio-pleistocene fault movement as evidence for mega-block kinematics within the Hyblean—Malta Plateau, Central Mediterranean. *Journal of geodynamics,* 19**,** 35-51.

Gentile, C. & Saisi, A. 2007. Ambient vibration testing of historic masonry towers for structural identification and damage assessment. *Construction and Building Materials,* 21**,** 1311-1321.

Gray, M. 2018. *Neolithic Temples of Malta* [Online]. Available: https://sacredsites.com/europe/malta/temples_malta.html [Accessed 2018].

Hibbitt, D., Karlsson, B. & Sorensen, P. 2012. Abaqus 6.12. 3 Manual. *Dassault Systèmes Simulia Corp., Providence, RI*.

Holland, T. 2018. *ADVANCED PREHISTORIC CULTURE* [Online]. Available: https://www.wondermondo.com/mnajdra/ [Accessed 28 November 2018].

Lanczos, C. 1950. *An iteration method for the solution of the eigenvalue problem of linear differential and integral operators*, United States Governm. Press Office Los Angeles, CA.

Layadi, K., Semmane, F. & Yelles-Chaouche, A. 2018. S-wave velocity structure of Chlef City, Algeria, by inversion of Rayleigh wave ellipticity. *Near Surface Geophysics,* 16**,** 328-339.

Leftheris, B., Sapounaki, A., Stavroulaki, M. E. & Stavroulakis, G. E. 2006. *Computational mechanics for heritage structures*, WIT Press.

Lourenço, P. B. 2002. Computations on historic masonry structures. *Progress in Structural Engineering and Materials,* 4**,** 301-319.

Malta, T. o. 2011. *Ħaġar Qim closed as wind rips shelter* [Online]. TimesofMalta.Com. Available: https://www.timesofmalta.com/articles/view/20110220/local/hagar-qim-closed-as-wind-rips-shelter.351112 [Accessed 7 October 2018].

Mele, E., De Luca, A. & Giordano, A. 2003. Modelling and analysis of a basilica under earthquake loading. *Journal of Cultural Heritage,* 4**,** 355-367.

Milani, G., Esquivel, Y. W., Lourenço, P. B., Riveiro, B. & Oliveira, D. V. 2013. Characterization of the response of quasi-periodic masonry: Geometrical investigation, homogenization and application to the Guimarães castle, Portugal. *Engineering Structures,* 56**,** 621-641.

News, G. 2009. *Mnajdra temples shelter suffers slight damage* [Online]. GozoNews.Com. Available: http://gozonews.com/7978/mnajdra-temples-shelter-suffers-slight-damage/ [Accessed 7 October 2018].

NUNISMAG. 2018. *2018 MALTA €2 commemorative coin dedicated to MNAJDRA temples* [Online]. Available: https://numismag.com/en/2018/01/18/2018-malta-e2-commemorative-coin-dedicated-to-mnajdra-temples/ [Accessed 28 November 2018].

Paige, C. C. 1972. Computational variants of the Lanczos method for the eigenproblem. *IMA Journal of Applied Mathematics,* 10**,** 373-381.

Panagiotopoulos, P. D. 1985. *Inequality Problems in Mechanics and Applications: Convex and nonconvex energy functions,* Boston, Basel, Stuttgart: Birkh¨auser Verlag.

Pellegrini, D., Girardi, M., Lourenço, P. B., Masciotta, M. G., Mendes, N., Padovani, C. & Ramos, L. F. 2018. Modal analysis of historical masonry structures: Linear perturbation and software benchmarking. *Construction and Building Materials,* 189**,** 1232-1250.

Ramírez-Cisneros, J., Lozano, J., Ferrer-Toledo, H., Rojas-Palacios, J., Vázquez-Rosas, R. & Mijares-Arellano, H. Dynamic behavior of Puebla City Cathedral. Proceeding of the 15th European conference on earthquake engineering, Lisbon, Portugal, 2012.

Ramos, L. F., Aguilar, R., Lourenço, P. B. & Moreira, S. 2013. Dynamic structural health monitoring of Saint Torcato church. *Mechanical Systems and Signal Processing,* 35**,** 1-15.

Reyes, E., Casati, M. & Gálvez, J. 2008. Cohesive crack model for mixed mode fracture of brick masonry. *International Journal of Fracture,* 151**,** 29.

Ridley, M. 1971. *The megalithic art of the Maltese islands*, (Beaulieu Ave., Christchurch, Hants.) Dolphin Press.

Sammut, S. 2016. *Lichen communities responses to a changing environment: A case study of Ħaġar Qim and Mnajdra Temples*.

Sánchez-Aparicio, L. J., Riveiro, B., González-Aguilera, D. & Ramos, L. F. 2014. The combination of geomatic approaches and operational modal analysis to improve calibration of finite element models: A case of study in Saint Torcato Church (Guimarães, Portugal). *Construction and Building Materials,* 70**,** 118-129.

Sepe, V., Speranza, E. & Viskovic, A. 2008. A method for large-scale vulnerability assessment of historic towers. *Structural Control and Health Monitoring: The Official Journal of the International Association for Structural Control and Monitoring and of the European Association for the Control of Structures,* 15**,** 389-415.

Simulia, A. V. 2013. 6.13 Documentation. *Dassault systemes*.

Spampinato, S., Ursino, A., Barbano, M., Pirrotta, C., Salvatore, R., Larocca, G. & Platania, P. R. 2017. *A Reappraisal of Seismicity and Eruptions of Pantelleria Island and the Sicily Channel (Italy)*.

Stavroulaki, M., Riveiro, B., Drosopoulos, G., Solla, M., Koutsianitis, P. & Stavroulakis, G. E. 2016. Modelling and strength evaluation of masonry bridges using terrestrial photogrammetry and finite elements. *Advances in Engineering Software,* 101**,** 136-148.

Stavroulaki, M. E., Drosopoulos, G. A., Tavlopoulou, E., Skoutelis, N. & Stavroulakis, G. E. 2018. Investigation of the structural behaviour of a masonry castle by considering the actual damage. *International Journal of Masonry Research and Innovation,* 3**,** 1-33.

Stavroulaki, M. E. & Liarakos, V. B. 2012. Dynamic analysis of a masonry wall with reinforced concrete lintels or tie-beams. *Engineering Structures,* 44**,** 23-33.

Taliercio, A. & Binda, L. 2007. The Basilica of San Vitale in Ravenna: Investigation on the current structural faults and their mid-term evolution. *Journal of Cultural Heritage,* 8**,** 99-118.

Terzi, V. G. & Ignatakis, C. E. 2018. Nonlinear finite element analyses for the restoration study of Xana, Greece. *Engineering Structures,* 167**,** 96-107.

Theuma, N. & Grima, R. 2006. The Megalithic Temples of Malta: towards a re-evaluation of heritage. *Managing World Heritage Sites***,** 263.

Tiberti, S., Acito, M. & Milani, G. 2016. Comprehensive FE numerical insight into Finale Emilia Castle behavior under 2012 Emilia Romagna seismic sequence: damage causes and seismic vulnerability mitigation hypothesis. *Engineering Structures,* 117**,** 397-421.

Tokimatsu, K. 1997. *Geotechnical site characterization using surface Geotechnical Engineering*.

Torpiano, A. 1995. The collapse and proposed restoration of a prehistoric megalithic structure. *WIT Transactions on The Built Environment,* 17.

Torpiano, A. 2011. *The engineering of the prehistoric megalithic temples in Malta* [Online]. [Accessed 28 Septemer 2018].

Türer, A., Aktaş Erdem, Y. D. & Güçhan, N. Ş. 2012. Reverse-Engineering Evaluation and Monitoring of Nemrut Monuments. *International Journal of Architectural Heritage,* 6**,** 373-395.

Ullah, I. & Prado, R. 2016. *The analysis of H/V curve from different ellipticity retrieval technique for a single 3c-station recording*.

Vannucci, S., Alessandrini, G., Cassar, J., Tampone, G. & Vannucci, M. L. 1994. *I Templi Megalitici Preistorici delle Isole Maltesi: cause e processi di degradazione del Globigerina Limestone*.

Vercher, J., Gil, E., Mas, A. & Lerma, C. 2015. Diagnosis and Intervention Criteria in Slabs Damaged by Severe Corrosion of Prestressed Joists. *Journal of Performance of Constructed Facilities,* 29**,** 04014040.

Vestroni, F., Beolchini, G., Antonacci, E. & Modena, C. Identification of dynamic characteristics of masonry buildings from forced vibration tests. Proceedings of the 11th world conference on earthquake engineering, 1996.

White, E. 2018. *Ten Tips for Visiting the Megalithic Temples of Malta & Gozo* [Online]. Available: https://archaeology-travel.com/travel-tips/visiting-the-megalithic-temples-of-malta-gozo/ [Accessed 24 Septmeber 2018].

Zanelli, A. 2015. 15 - Architectural fabric structures in the refurbishment of archaeological and cultural heritage areas. *In:* de Llorens, J. I. (ed.) *Fabric Structures in Architecture.* Woodhead Publishing.

Živanović, S., Pavic, A. & Reynolds, P. 2006. Modal testing and FE model tuning of a lively footbridge structure. *Engineering Structures,* 28**,** 857-868.